Materials and Design 196 (2020) 109093

Contents lists available at ScienceDirect

Materials and Design

journal homepage: www.elsevier.com/locate/matdes

A review of non-destructive testing techniques for the in-situ investigation of fretting fatigue cracks

Y. Kong, C.J. Bennett *, C.J. Hyde

Gas Turbines and Transmissions Research Centre, Faculty of Engineering, The University of Nottingham, Nottingham NG7 2RD, UK

HIGHLIGHTS

- A review on recent non-destructive techniques that have been used in-situ with fretting fatigue tests for crack detection.
- Comparisons of the sensitivity, the number of cycles to crack nucleation detection and capability of techniques.
- Recent developments in non-destructive techniques applicable to fretting fatigue.

GRAPHICAL ABSTRACT

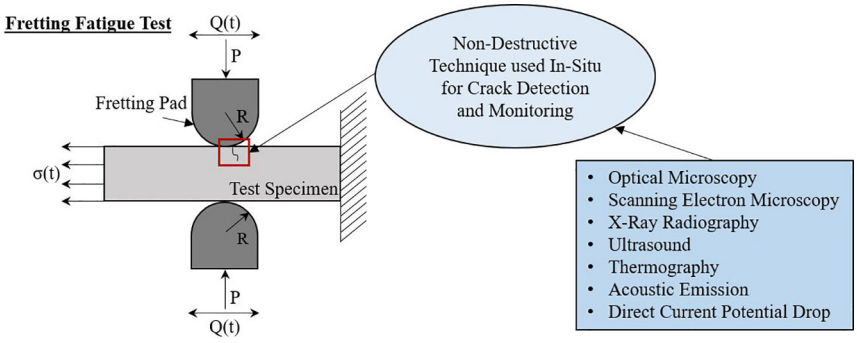

ARTICLE INFO

Article history:
Received 6 December 2019
Received in revised form 11 August 2020
Accepted 22 August 2020
Available online 29 August 2020

Keywords:
Fretting
Fatigue
Cracks
In-situ
Non-destructive testing
Review

ABSTRACT

Fretting fatigue can significantly reduce the life of components, leading to unexpected in-service failures. This phenomenon has been studied for over a century, with significant progress being made during the past decade. There are various methods that have been used to study fretting fatigue cracks in order to gain a greater understanding of the effects of fretting fatigue. Destructive methods are traditionally used to observe fretting fatigue cracks. Although useful in determining crack location, crack length, crack propagation modes, crack path and shape, it is not efficient or reliable for time based measurements. Non-destructive testing has developed in recent years and now in-situ monitoring can be used during testing in order to increase the understanding of fretting fatigue. This paper presents a review of non-destructive testing techniques used in-situ during fretting fatigue testing, which are compared in order to conclude the suitability of each technique. Recent developments in non-destructive techniques that could be also applied for fretting fatigue tests are also discussed, as well as recommendations for future research made.

Contents

* Corresponding author.
E-mail address: epzcjb@exmail.nottingham.ac.uk (C.J. Bennett).

https://doi.org/10.1016/j.matdes.2020.109093

1. Introduction

Fretting fatigue is a failure mechanism that occurs due to contacting components experiencing small relative displacements while being subjected to cyclic bulk stress. This phenomenon has been studied for over a century, dating back to 1911 [1]. Some examples of applications that experience fretting fatigue include dovetails [2–4] and spline couplings [5] in gas-turbine aero-engines, railway axles [6–8], bolted joints [9,10] and overhead conductors and wires [11–14].

A common set up for a simple fretting fatigue test involves using a pad rubbing on a flat surface. Fig. 1 shows a schematic of a cylinder-on-flat fretting fatigue test set-up with a cylindrical pad with a radius, R; a normal force, P, to create the contact; a cyclic traction force, Q, to create the relative displacements; a bulk stress, σ for the fatigue loading and a contact width, $2a$.

Under fretting, there are two sliding regimes known as the partial slip regime and the gross slip regime. For fretting fatigue testing, the tests are set up in the partial slip regime as this increases the likelihood of the initiation of fretting fatigue cracks, the primary focus of this review, whereas the gross slip regime (larger displacements) leads to the formation of wear debris and fretting wear dominates [15]. This relationship between slip amplitude, fatigue life and wear rate was shown by Vingsbo and Söderberg [16,17] and is summarised in Fig. 2. At low slip amplitude, the wear rate is low and there is little effect on fatigue life; as the slip amplitude increases in the partial slip regime, the fatigue life falls and there is a small increase in wear rate. At the transition between the partial and the gross slip regimes, the fatigue life reaches its minimum. As slip amplitude increases further, the wear rate increases rapidly, while the fatigue life starts to increase again as fatigue cracks are worn away before they can propagate. It should be noted that other pad configurations include a bridge configuration, which includes two feet with a gap in between. In this configuration, the slip is governed by the elastic deformation of the specimen between the pads under the applied bulk stress. The slip regime is often unknown, however, as the contact of one foot tends to slip before the other [18].

For gross sliding, the contact shear distribution is a parabola with no stick zone. The partial slip regime involves a mixture of stick and slip behaviour, as presented in Fig. 3 for a cylinder-on-flat configuration. A reduction in the shear distribution occurs within the stick zone. For plain fretting, the stick zone is quantified between −c and c and the contact shear stress distribution is symmetrical (derived from Mindlin [17]). For fretting fatigue, the bulk stress causes a shift in the stick zone, on the gross sliding parabola, from the strain induced in the flat specimen [17]. This shift is characterised by the eccentricity, e, which changes the stick zone to lie between −c+e and c+e. The shear stress distribution becomes asymmetric and the maximum shear value appears on the trailing edge of the stick zone at −c+e, where the bulk stress is applied. Many experimental tests have reported crack initiation being located at the trailing edge of the contact zone [19–22].

From the combination of fretting loads in the partial slip regime and the additional bulk stress, cracks initiate at the contact. Crack initiation and crack propagation causes failure due to fretting fatigue. The fretting load causes mode II crack initiation and early crack propagation. As the crack propagates further, the bulk stress dominates and causes mode I crack propagation. This consequently leads to failure earlier than

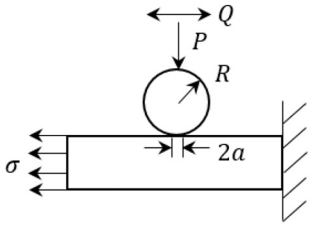

Fig. 1. Cylinder-on-flat fretting test schematic.

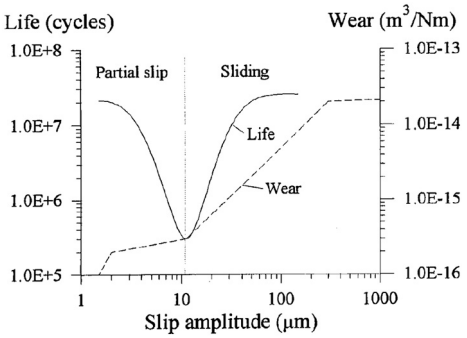

Fig. 2. Relationship between slip amplitude with fatigue life and wear rate [17].

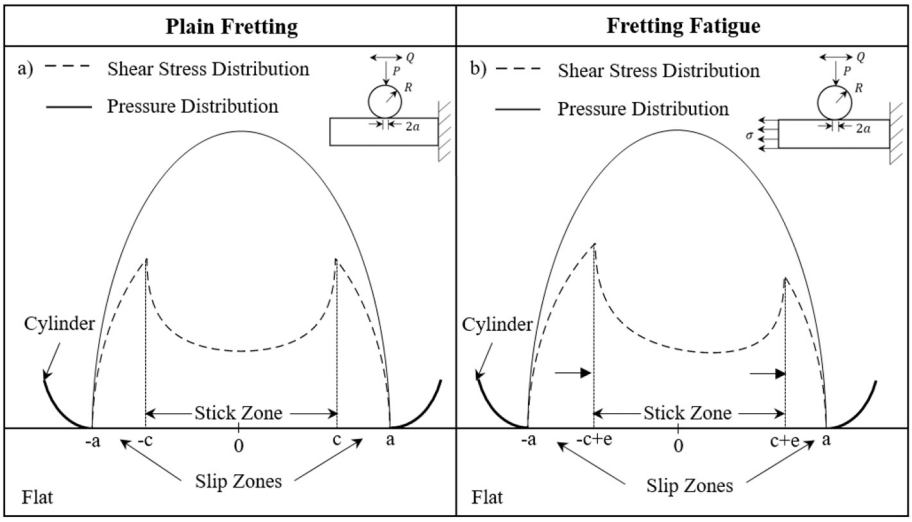

Fig. 3. Contact shear stress distributions for cylinder on flat contact in the partial slip regime under a) plain fretting and b) fretting fatigue.

expected based on the plain fatigue limit of a material. Crack initiation is associated with the accumulation of damage from the start of loading until a crack forms [17,23]. There are two main definitions for crack initiation: one for an experimental approach and one for a mechanics approach. Experimentally, crack initiation is defined as either when a crack is detected up to a specified size or when a crack is first detected and crack propagation is defined as the crack growing after this period. The mechanics approach refers crack initiation to the period prior to crack propagation, which cannot be described by fracture mechanics. This period typically involves the formation of a crack with a length the size of a few grains [17].

An extensive amount of research has been dedicated to modelling crack initiation and crack propagation behaviour. This involves predicting the crack initiation and propagation lifetimes [24–46], crack paths and orientations [28,29,40,47–55], crack locations [24,28,29,38,40–45,50,56,57] and the crack growth rate [36,37,52,58,59]. Fretting fatigue crack initiation criteria is often used to predict crack initiation life, orientation and location. This can be split into four approaches [23]: critical plane approach, stress invariant approach, continuum damage mechanics approach and fretting specific parameters. The critical plane approach defines parameters that are developed on the basis that failure occurs on planes prone to failure. Some examples include, Araujo and Nowell [39] using an averaging method with the Smith-Watson-Topper (SWT) and the Fatemi-Socie (FS) parameters to predict initiation life for a cylinder-on-flat fretting fatigue test. The authors suggested for more accurate predictions, a model that includes the material microstructure should be involved. Sum et al. [40] expanded this model by incorporating with a finite element (FE) model for a cylinder-on-flat configuration and for a spline coupling. This allowed to predict crack initiation location and orientation, as well as lifetime. McCarthy et al. [36] used the SWT parameter and used crystal plasticity to capture a more accurate prediction of crack initiation life, location and orientation. Other models include using an FE model to include incremental wear with the SWT parameter to improve the prediction of crack initiation life and location [41], as well as using the SWT and FS parameter with a variable initiation length technique to improve the prediction of crack initiation angle [54,55]. Another critical plane approach includes the Modified Wöhler Curve Method (MWCM), which have also been compared with SWT and FS parameters in its prediction for total life for a cylinder-on-flat [32,33] and overhead conductors [33], which was combined with an FE model and the inclusion of incremental wear removal; and early crack path and orientation [47]. Other critical plane approaches have been compared for crack initiation life and orientation in works of Bhatti and Wahab [27].

The stress invariant approach defines parameters that are based on the stress invariant, which are used to define the failure of a material. The Crossland parameter is a fatigue limit criterion for multiaxial stress conditions and is mainly used for fretting fatigue problems [23]. The parameter has been used to predict the risk of crack initiation and its location [45,46,57].

The continuum damage mechanics approach defines parameters based on damage mechanics, which are used to define the damage of a material. This approach has only been used to predict crack initiation lifetimes, which have correlated well with experimental results [26,29,30,56].

Fretting specific parameters are based on incorporating the slip amplitude for a fretting fatigue test. These include the Ruiz parameters and fretting damage parameter. It was found that the Ruiz wear parameter was unable to capture crack initiation, whereas the Ruiz initiation parameter was able to capture crack initiation location well, but unable to capture cycles to crack initiation compared with experimental data [38]. Ding et al. [42] modified the SWT parameter to incorporate the Ruiz wear parameter to take into account the wear effects. This was shown to provide a good correlation of initiation life and location with experimental results for different geometries [42–44]. For further information, Bhatti and Wahab [23] reviews the fretting fatigue crack initiation criteria in detail.

The most common crack propagation modelling involves the uses of short crack growth and linear elastic fracture mechanics (LEFM). These are modelled to predict the crack growth rate for short crack growth (mode II) and LEFM predicts the crack growth rate for long crack growth (mode I). LEFM involves the use of the Paris and Erdogan [60] relationship for stable crack growth, which assumes that the stresses around the crack tip are elastic. For short crack growth, LEFM cannot be applied due to the plasticity around the crack tip. Therefore, it is commonly modelled using the El Haddad model [18,61], who modified the Paris and Ergdon [60] relationship to accommodate for short crack growth behaviour. It has been used to account for life during this period [34,35,37,59]. Other methods for modelling short crack growth include the microstructural approach (known as the Navarro-Rios model). De Panemaecker et al. [59] compared the short crack growth approach with the microstructural approach to capture the short crack growth rate for fretting fatigue. It was found that the microstructural approach captured the short crack growth rate closer with experimental results. Life for long crack growth has also been predicted using LEFM [29,37], as well as its crack growth rate [53].

To model the crack path and orientation, multiaxial crack propagation criteria are mainly used used. One criterion includes the maximum tangential stress criterion (MTS), which considers a crack propagating at the crack tip in the radial direction [51]. This has been used with a FE model to predict the crack angle [19]. This has also been used to define the crack path, but has been found that it is not the most suitable criterion when compared with experimental or validation data [29,51,53]. Martinez et al. [51] and Marco et al. [49] showed that the minimum shear stress range criterion combined with an extended FE model (XFEM), where propagation will occur at an angle where the mode II stress intensity factor range is at a minimum, presented acceptable results of the crack path with experimental data. Other criteria include mode I crack growth rate, stress intensity factor and its range being at a maximum [52,53] to model the crack orientation and path. These were incorporated with an extend FE model and showed to have a good correlation with experimental 2D crack paths.

1.1. Destructive techniques for crack analysis

Experimental observation of fretting fatigue has increased in recent years with the aim of obtaining a greater understanding of the fretting fatigue and crack growth behaviour of materials, and to collect data in order to produce predictive tools for use in more complex geometries or loading cases through the use of analytical and numerical modelling approaches. Traditionally, this has involved the use of destructive techniques. Destructive testing involves optically analysing a specimen when it reaches failure or optically analysing an unbroken specimen from an interrupted experiment by sectioning the specimen and observing cracks/defects. For specimens that experience fretting fatigue, tests are interrupted at a certain point in time and the specimen is sectioned in the middle of its fretting scar, as shown in Fig. 4, and its surfaces polished. The projected crack length, b_p, can then be measured at the specimen's cross section, typically, using an optical microscope. Polishing and observation steps are typically repeated three times to both contacting specimens in the test to find the maximum projected crack length [22,45,62–65].

The projected crack length can be used to obtain the crack nucleation fretting load threshold. Carrying out this experiment for different fretting load amplitudes with a constant number of cycles, the maximum projected crack length ($b_{p,max}$) can be determined. Once the maximum projected crack length reaches zero, i.e. no crack is observed, the crack initiation tangential load threshold can be found [15,22,45]. The projected crack length is assumed to be linear with the fretting load and the intersection with the fretting load axis ($Q^*/\mu P$) is where the crack nucleation threshold is identified (Q^*_{CN}), as shown in Fig. 5a. This can be used for different fretting loads and can be plotted against the bulk stress (σ_F) to obtain a fretting crack nucleation boundary [45] (as shown in Fig. 5b).

Further information can be obtained from the destructive method. From obtaining scanning electron microscopy (SEM) images, crack initiation sites can be found as well as crack growth paths, crack shapes and crack propagation modes [22,24]. Furthermore, by using a confocal microscope, angles for crack initiation and for early crack paths can be found [24], allowing crack propagation modes to be identified. To monitor crack propagation, a fretting fatigue test is repeated a number of times, each using a different specimen, stopping the test at a different number of cycles [66]. The crack length is measured for each specimen and can then be characterised as a function of the number of cycles. This can, due to the inherent variability in the crack initiation and growth between specimens, give an inaccurate representation of how a crack propagates under any given test condition.

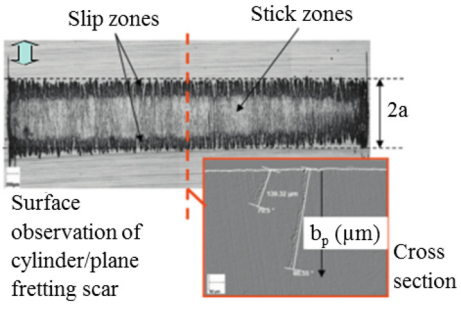

Fig. 4. An image of the destructive method [22].

Overall, the destructive method can gain information on the crack location, crack length, crack propagation modes, crack path and shape. Limitations of this technique are that it is time consuming with regards to time based measurements, its destructive, only discrete data points are produced and that specimens cracks can only be observed after a test has failed or interrupted. Also, it is not possible to monitor what is happening during the fretting fatigue test. Therefore, recent years have seen attempts to use non-destructive testing (NDT) techniques for in-situ crack detection and crack growth monitoring during fretting fatigue testing to obtain more information about cracks during fretting fatigue tests in a more efficient manner.

1.2. Non-destructive testing techniques

Non-destructive testing (NDT) techniques involve monitoring methods that are used to test a material without damaging the specimen being tested. Such testing techniques are commonly used for inspecting a material for defects or flaws without having to destroy the specimen. Another use of NDT techniques is to measure the mechanical properties of a material [67] such as, Young's modulus from ultrasound velocities [68] and determining grain size during thermomechanical processing using laser ultraound by measuring the ultrasound attenuation [69]. Another application includes determining the coefficient of friction using digital image correlation by measuring the relative amplitude of displacement between contacting surfaces [29]. The main advantages of using such NDT techniques include the adaptability with being able to use them in-situ with various types of mechanical tests which significantly advances the knowledge of how materials behave with time. For fretting fatigue, the main requirements for evaluating cracks from NDT techniques involve obtaining data for the cycles to crack initiation, monitoring crack growth, identification of the crack propagation modes, monitoring the crack growth paths, monitoring the crack shape and the detection of crack locations. NDT techniques that have previously covered one or more of these requirements for in-situ fretting fatigue testing include optical microscopy, SEM, X-ray radiography, ultrasound, thermography, acoustic emission, direct current potential drop methods. The advantages and limitations of using these techniques are presented in Table 1.

Recent advances in NDT techniques and sustained interest in fretting fatigue has led to the requirement for the current state of knowledge to be reviewed in order to assess the suitability of these NDT techniques for in-situ fretting fatigue tests. Conclusions are drawn with a view to inform challenges and future research directions.

2. Non-destructive testing techniques for crack detection and growth monitoring of fretting fatigue tests

NDT techniques are appropriate methods for quantifying crack behaviour during mechanical testing (including fretting fatigue testing) without damaging the test specimen. There are many possible NDT techniques that can be used, in-situ, during fretting fatigue testing. This includes: Optical Microscopy (OM), Scanning Electron Microscopy (SEM), X-Ray Radiography (XR), Ultrasound, Thermography, Acoustic Emission (AE) and Direct Current Potential Drop (DCPD) techniques.

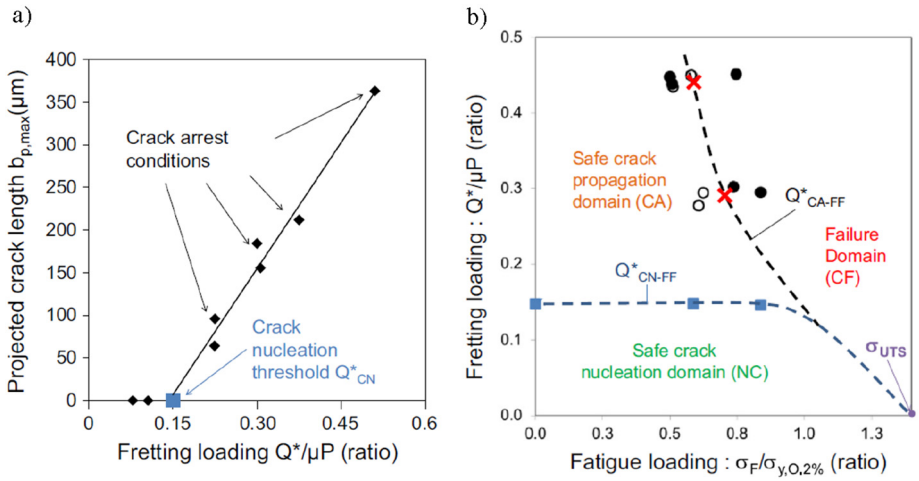

Fig. 5. a) Crack nucleation fretting load threshold. b) Crack nucleation boundary for fretting fatigue achieved by a destructive method [45].

2.1. Optical microscopy

Optical microscopy (OM) involves an optical microscope, which is a microscope that uses visible light to magnify regions of interest to inspect features, such as cracks, by the use of lenses. The microscope is connected to a computer, where two-dimensional images of the cracks can viewed with a spatial resolution up to 200 nm [82]. An example of an image is presented in Fig. 6, where it can be seen that crack initiation occurs near the trailing edge of contact. When used in-situ with a fretting fatigue test, there have been three of methods used for experimental set-up. Jeung et al. [75] positions the optical microscope to view the contact area and uses a light to illuminate the area. Tests are interrupted to focus and capture images of a developing crack, as well as the measure crack length of a crack. Another method includes pausing the test and using a replica, which is a film that is positioned over the crack and acetone is added to the crack, revealing crack features onto the film [37,73,74,105–108]. The replica is then examined under an optical microscope, where the crack length is measured. The final method used is known as video microscopy, which involves using an optical microscope and filming the contact area between the specimen and pads during the test [70,71]. The test is also paused to scan and focus the region of interest to capture images and measure crack lengths.

The main advantages of using any of these methods are that a visual of the crack location, crack shape and crack path can be obtained, and the evolution of the crack length has successfully been found with number of cycles [37,70,71,73–75,105–107]. Arora et al. [70] used a video microscope for flat on flat fretting fatigue tests and compared the crack growth for various loading parameters. The tests were repeated three times for each loading condition, which showed that the crack length with respect to the number of cycles was consistent and repeatable. Additionally, crack growth has also been monitored for specimens with different surface modifications and at temperatures of 100 °C and 200 °C. It is, also, possible to obtain a crack initiation lifetime [37,70,71,73,74]. This is determined by pausing the test and observing the region of interest using an optical microscope until a crack appears. Therefore, this approximation is highly dependent on the imaging frequency and image resolution. It has been found that by optimising the imaging frequency, the results in detecting a minimum crack length are more consistent. Crack initiation and growth measurements have, also, been successfully used to compare or assist modelling these in-situ experimental results, such as using the finite element method (FEM) to predict residual stresses and surface roughness for different surface modifications [37,73]; and predict crack propagation lifetime and in turn predict crack initiation lifetime based on experimental cycles to failure [74]; and to predict crack initiation lifetime based on strain energy density critereon and crack propagation life time using the crack analogue model, which was compared with experimental results [71].

Although there are many advantages, there are many limitations to consider. This includes designing the fretting fatigue test to ensure the initiation of surface cracks as an optical microscope is only capable of capturing these. Furthermore, the crack initiation location needs to be known prior to the measurements and images being taken, which involves optimising the frequency of the tests being paused. This may be achieved by repeating tests and finding how often tests need to be paused until crack initiation can be found. Some design considerations include that for an optical microscope the region of interest needs to be in the order of millimetres [72,82] and therefore, specimens and test set-ups need to be small to use this technique to obtain high quality images. Also, it needs to be ensured that there is a well illuminated field of view and that the specimen is polished to enhance the contrast to detect a crack [72].

2.2. Scanning Electron microscopy

Scanning Electron Microscopy (SEM) is a type of microscope, which allows the visualisation of microscopic features not visible to the human eye. It differs to an optical microscope, which uses light to form images, instead, it uses an electron beam. This allows details smaller than 1 nm to be seen, as its wavelength is much smaller compared to that of visible light [82]. The electron beam from the electron source is scanned across a rectangular region of interest of the specimen within a vacuum and the interaction causes various forms of energy dissipation. This can be picked up by detectors and used to form data and greyscale images, which are then processed by a computer. The main detected signals include [82]:

- secondary electrons, which produce morphology and surface topography images, as less electrons leave flat surfaces and visa versa;
- backscattered electrons, which produce atomic number and grain boundaries imaging due to the number of reflected electrons varying between atoms giving contrast;
- electron backscattered diffraction, which gives pattern images of the crystallographic orientation of grains and phase identification;
- and energy dispersive x-ray spectroscopy (EDS) gives elemental analysis information and X-ray maps.

Fig. 7 shows the typical set-up of a SEM with its detectors for analysing a specimen.

SEM has been used in-situ with many experiments, such as fatigue [109–114] and fretting wear [115], as well as fretting fatigue experiments [76–81,116]. To use SEM in-situ, the tests usually require a fixture

Table 1
The advantages and Limitations of NDT techniques used in the detection of cracks for fretting fatigue.

NDT Technique	Refs.	Description	Advantages	Limitations
Optical Microscopy	[37,70–75]	An optical microscope is directed towards the region of interest or replica and microscopic images are captured of the crack	• A contactless technique • Visual • Locate crack initiation • Obtain number of cycles to crack initiation • Monitor crack evolution • Obtain crack length with number of cycles • Obtain crack path • Simple to use and readily available • Tests can be adapted for higher temperatures with the use of a replica	• Only captures surface cracks • Well illuminated field of view is required • Crack initially needs to be located before measurements and images can be taken • Smaller specimens are required to ensure area of interest is within the field of view
SEM	[76–83]	An electron beam is scanned over the surface of a specimen during a test and an image of its microstructure is produced from the response signals	• A contactless technique • Visual • Determine crack location and monitor path • Monitor crack length • Determine the cycles to crack initiation • Identify crack propagation modes • Obtain microstructural features, such as slip lines • Tests can be adapted for high temperature tests	• Space constraints of samples due to the test having to be adapted to fit within vacuum chamber • Tests need to be interrupted for image capture • Detects only surface and subsurface cracks in plane of view • Smaller specimens are required to ensure area of interest is within the field of view
X-Ray Radiography	[59,67,84,85]	An X-ray source penetrates specimen onto an X-ray imaging detector	• A contactless technique • Detects internal and surface cracks • Visual • Can be used for various geometries and materials • Determine crack location • Identify crack propagation modes • Monitor crack length • Determine the cycles to crack initiation	• Expensive • Large and complex equipment with limited access • Fretting fatigue tests need to be interrupted to obtain radiographs • The user needs to be experienced • Specimens and test specimens need to be small to fit within the required space and capture a high image resolution
Ultrasound	[10,67,84,86–89]	Use of ultrasonic waves into a specimen and measuring the wave response	• Can detect the presence of cracks without direct access to the region of interest • Detects internal and surface cracks • Ultrasound probes can be designed for complex geometries • Determine the cycles to crack initiation	• Approximate crack location needs to be known • Difficult to inspect materials with low sound transmission • There needs to be access to the surface to transmit the ultrasound • Transducer needs to be in contact with the surface or through a fluid • Cracks planar and parallel to the ultrasound wave propagation may go undetected
Thermography	[90–95]	An infrared camera is used to observe the temperature change in a specimen	• A contactless technique • Detect crack initiation due to temperature increase at the crack tip • Determine crack location • Crack lengths can be measured • Determine the cycles to crack initiation • Thermal visual • Cracks can be scanned over a large area	• Temperature rise needs to be high enough at the crack tip to be detected • Can only detect cracks up to a limited thickness below the surface of the material • Crack location can be difficult for complex contacting geometries
Acoustic Emission	[66,84,96–100]	Acoustic emission waves are picked up by a sensor from displacements within a specimen	• Real time monitoring of crack initiation and propagation • Determine crack location • Determine crack propagation modes • Do not need direct access to the crack • Determine the cycles to crack initiation • A volume of material can be monitored without the need for scanning • Can detect internal cracks and defects	• AE signal produces a lot of scatter due to noise • The user needs to ensure the signal is interpreted correctly
Direct Current Potential Drop (DCPD)	[45,46,59,62,65,101,104]	Two probes are used to measure the voltage across a region of interest, where a DC current is passed through the circuit and the potential difference is measured	• Detect crack initiation and propagation • PD results can be correlated to the crack length • Determine crack propagation modes • Determine the cycles to crack initiation	• Approximate crack location needs to be known • Surface must be accessible • PD measurements can produce scatter due to the contact

to fit within the vacuum chamber. For fretting fatigue experiments, this is particularly challenging, as there are loads in two directions and need a requirement to make sure the region of interest is in field of view for SEM [76–81]. A typical fixture for fretting fatigue experiments is shown in Fig. 8a, where a bridge configuration was used with cylindrical feet. Additionally, the device dimensions had to be adapted to fit within the vacuum chamber.

SEM images are obtained by pausing the test to scan the region of interest and images are taken. An example of SEM images from Han et al. [77] are presented in Fig. 9 showing the inititation of secondary cracks. These images have been used to investigate crack initiation sites, the evolution of a crack with respect to number of cycles and evolution of crystallographic slip systems relative to fretting fatigue cracks [76–80] for a nickel-based single-crystal superalloy (NBSX) for different

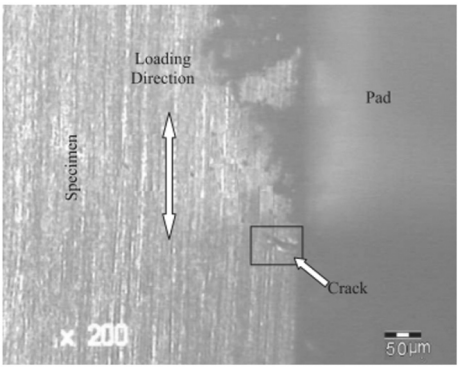

Fig. 6. Image of crack initiation detection using a video microscope [71].

crystallographic orientations, as well as investigating the effects of relative slip [81]. Further investigations include observing the evolution of cracks with respect to the final dislocation density [80] and monitoring subsurface crack growth [77]. These tests were for fretting fatigue experiments that only involved a normal loading and cyclic bulk stress, and did not include tangential loading.

In addition, it is possible to adapt the fretting fatigue experiments to allow them to be carried out at higher temperatures. Su et al. [76] created a chamber with a viewing hole to contain the heated (400 °C) specimen within the SEM vacuum chamber. Although not investigated in previous fretting fatigue experiments, it is also possible to measure crack length with number of cycles [112,114], as Zhang et al. [114] found for an in-situ SEM with fatigue experiment for notched dogbone specimens with different hydrogen contents at room temperature and at 300 °C. Fatigue tests that have been carried out also prove that it is possible to reach temperatures up to 1000 °C with further modifications [111].

Desipte the many advantages, there are many limitations to consider with in-situ studies using SEM. There are space constraints, where specimens need to be small enough to fit within the vacuum chamber [76–80,117,118], as well as the region of interest has to be in the size range of micrometres to millimetres [82]. Furthermore, it is not possible to observe internal cracks, as this technique is restricted to investigating surface cracks and cracks several micrometres deep [82]. Tests, also, need to be interrupted in order to scan the region of interest and take SEM images. This can take around 60 s to complete [119]. Therefore, tests need to be taken into account for interruption and if an experiment is based on investigating crack initiation, then an optimum frequency of interruptions need to be found [117] (as in OM). For fretting fatigue tests in the literature, the imaging frequency is not reported and the minimum crack size found ranges from 1 μm [77] to 133 μm [76].

2.3. X-ray radiography

This technique involves a specimen being placed between an X-ray source and an X-ray imaging detector. Examples of imaging detectors include X-ray films [93], which produce a radiograph onto a film, as shown in Fig. 10, and digital detectors, such as charge coupled devices (CCDs) [120], which digitally processes an image onto a computer. The X-ray source penetrates through the specimen on to the detector as a straight line. Some of the radiation is absorbed by the specimen, which produces an internal image of the specimen showing defects and cracks within the material. This has the benefit that both surface and internal cracks (cracks that initiate from a surface of a specimen to cracks that initiate internally within a specimen) can be detected using this method [67].

The main advantage of this technique is that it provides a physical image, which can be measured. De Pannemaecker et al. [59,85] used this technique in-situ with a cylinder-on-flat fretting fatigue test (as shown in Fig. 11) to monitor crack initiation and crack growth. The fretting fatigue test was interrupted every 5000 fretting fatigue cycles in order to take an X-ray image of the specimen, as shown in Fig. 12, allowing the number of cycles to crack initiation to be determined with a tolerance of ±5000 fretting fatigue cycles, as well as the crack

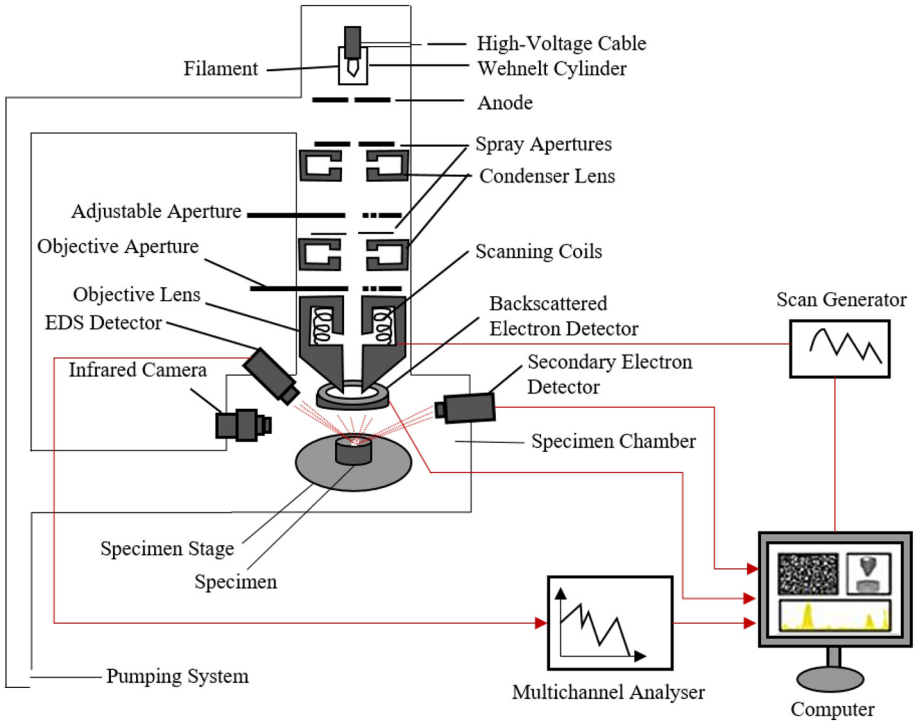

Fig. 7. Set-up of analysing a specimen using SEM (adapted from [82]).

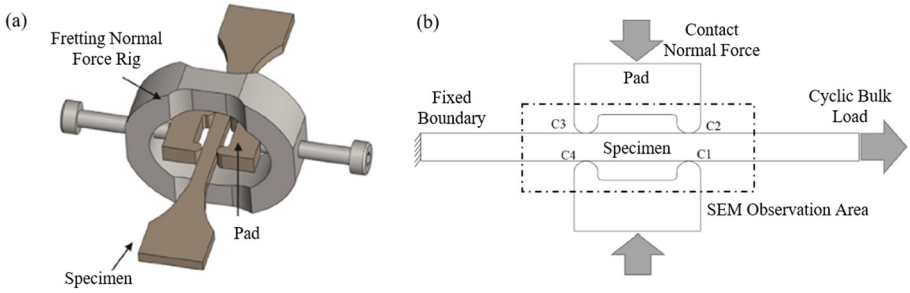

Fig. 8. (a) Fretting fatigue fixture for in-situ SEM and (b) a schematic of the specimen, pads and loading [78].

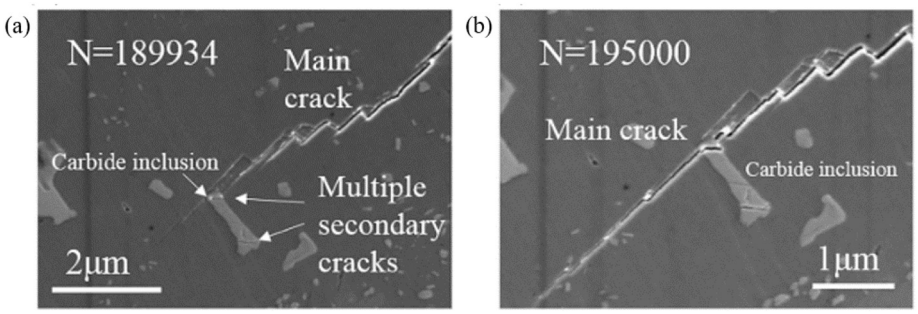

Fig. 9. SEM images of a secondary crack initiation for (a) a general view and (b) a zoomed in view [77].

initiation location to be defined. As the crack propagated, the crack length was measured every 5000 fretting cycles from the subsequent images and the crack path and shape was identified. In addition, the images allowed the different crack propagation modes to be identified, as shown in Fig. 13. This technique also allowed data on short crack growth to be obtained, which can be used to define crack propagation modes. In order to have access to the high energy x-rays required to achieve time-resolved x-ray imaging with sufficient spatial resolution (a voxel size of $<1\ \mu m$), the authors used a synchotron imaging beamline as opposed to standard laboratory x-ray radiography equipment [85,121]. This also allowed a larger distance between the specimen and the source, which gives the ability to enhance the phase contrast in the radiographic images increasing the visibility of smaller defects [122,123].

Although the data generated by this technique is extensive and useful, there are many limitations. This technique involves expensive, large and complex equipment with limited access, which requires the user to have expertise with using this equipment [67,84,124]. In addition, the fretting fatigue test has to be interrupted at defined points throughout the test to obtain the radiographs, which may affect the test and specimen, potentially reducing the reliability of the results, similar to OM and SEM. Furthermore, there are design considerations to take into account. Due to a small required voxel size, this means access to a high energy synchrotron beamline is required to achieve the required high quality images. The duration of the beam-time for De Pannemaecker et al. [59,85] was 24 h, which limited the test by how many cycles could be run. Also, due to the required voxel size, this meant scans were performed on a small area to achieve a high resolution and hence, limiting the specimen and device sizes.

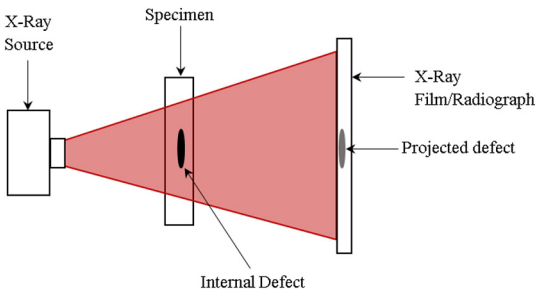

Fig. 10. X-ray radiography method schematic.

2.4. Ultrasound

Ultrasound testing involves inputting ultrasound waves into a specimen and recording the receiving wave response. Ultrasound waves are directed to a region of interest where a crack is expected to occur and changes in the receiving wave response can identify defects within the material. There are two main types of utrasound inspection known as through-transmission ultrasound and pulse-echo ultrasound [84,86] (see Fig. 14). Through-transmission ultrasound involves the use of two

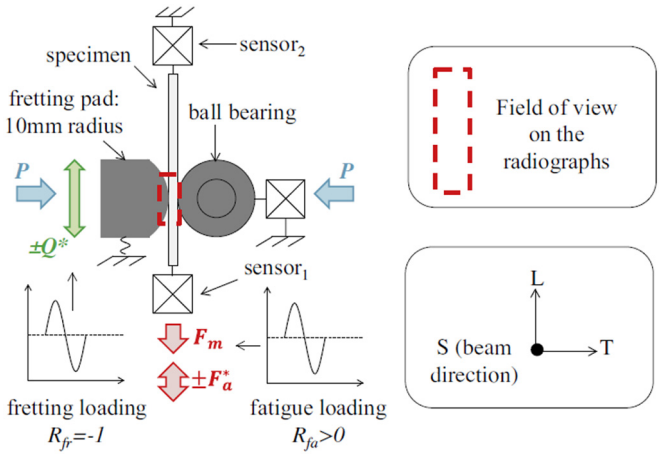

Fig. 11. De Pannemaecker et al. [85] set up for an in-situ fretting fatigue test with X-ray radiography.

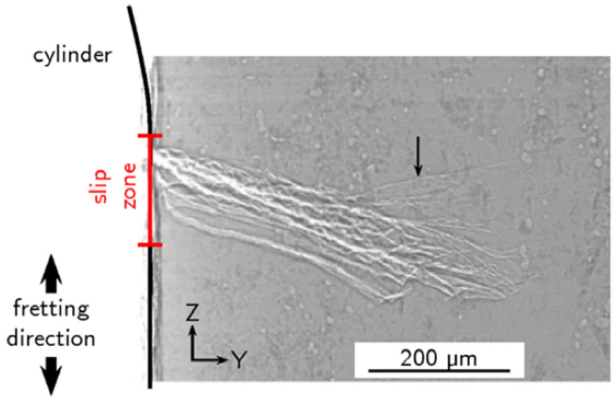

Fig. 12. An example of a 2D radiography showing a fretting fatigue crack [122].

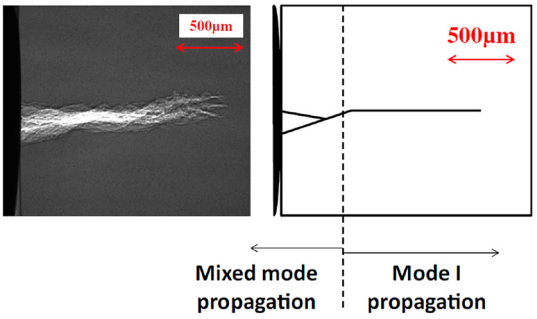

Fig. 13. Distinguishing modes of fretting fatigue crack propagation using X-ray radiography [85].

transducers placed either side of the specimen: a transmitter to generate the ultrasound; and a receiver to receive the ultrasound on the opposite side of the specimen. Pulse-echo ultrasound only uses one transducer, which acts as both the transmitter and the receiver. This transducer transmits the ultrasound and receives the reflected wave response.

The presence of fatigue cracks during fretting fatigue testing have been identified with this technique without direct access to the region of interest, which is particularly advantageous for fretting fatigue tests [10,87–89]. Changes in the amplitude and shape of the ultrasound wave response shows a presence of a crack being detected. One method for reaching the contact area of fretting fatigue tests, includes the use of coupling wedges to convert the ultrasound waves from longitudinal waves to shear waves by changing the angle of the ultrasonic transducer. This changes the direction of the ultrasound wave propagation and causes the particles of the medium to vibrate perpendicular to the direction of the ultrasound wave propagation [67,87–89]. This method involves using pulse-echo inspection and the reflected shear wave shows a crack has been detected, as presented in Fig. 15. Hutson et al. [87] was able to report the cycles to crack initation using this method for high normal loads. In addition, this method has been shown to be capable of detecting fretting fatigue cracks for more complex geometries such as teeth and wedge dovetails on a rotor shaft for an electrical power generator [89]. Another method that has been applied to fretting fatigue is the use of pulse echo inspection with longitudinal waves using a water bag [10,125], as shown in Fig. 16. This allows surface acoustic waves (SAW) to be penetrated through the water bag and a fretting fatigue crack to be detected from a distance away from the region of interest. Wagle et al. [10,125] used this method for analysis of the behaviour of bolted joints between aluminium alloy plates, showing a practical example of using this technique. It was found that there was a steep increase in the intensity of the SAW upon the initiation of a crack and that the intensity continued to increase as the crack length increased. Initially, tests were interrupted to take SAW meaurements [10], but later this was automated by the authors [125]. Despite the mechanical noise from fretting fatigue tests, the presence of cracks has still been detected from new peaks observed in the ultrasound waveform [10,88,89].

A limitation of using ultrasound, in comparison with other techniques, is that its sensitivity is low for detecting crack initiation. This means that the number of cycles to crack initiation is detected at longer crack lengths, as the crack length needs to be large enough (>200μm [10,87]) to be detected using ultrasound; furthermore, Hutson and Stubbs [88] showed that it is difficult to identify short crack lengths during a fretting fatigue test due to various sources of noise within the system, which suggests that shorter cracks may go undetected. Therefore, it is important to filter out acoustic and electromagnetic noise efficiently [88,126]. Additionally, if a crack is planar and parallel to the direction of ultrasound wave propagation, the crack may also go undetected [84,86,124], as the receiving wave response is not large enough to be detected. Furthermore, ultrasound transducers need to be attached to the specimen and the signal needs to be directed towards the approximate area of the crack location. During situations of parts undergoing fretting fatigue with complex geometries, the crack location is not always known, making this technique difficult to use for these applications. Also, any material that has low sound transmission, has high signal to

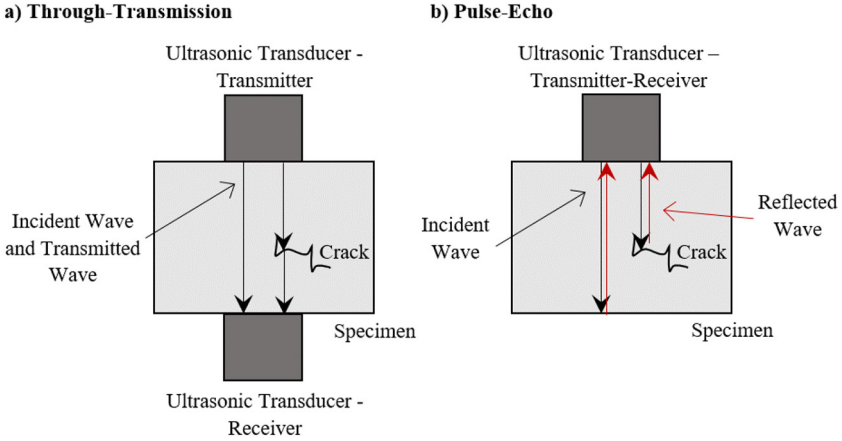

Fig. 14. Schematic of a) through-transmission and b) pulse-echo ultrasound methods.

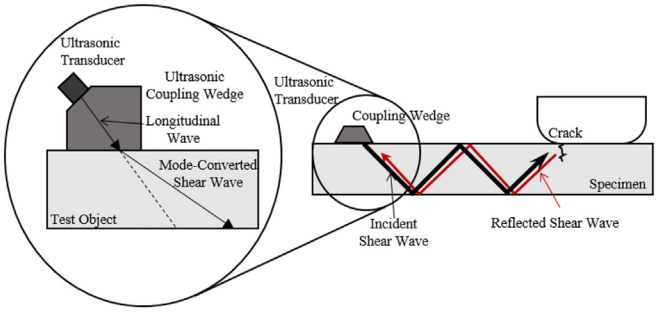

Fig. 15. Longitudinal wave to shear wave conversion to reach the fretting region of interest (adapted from [88]).

noise ratio, is heterogeneous, as well as specimens that have rough surfaces, small and thin geometry or are irregular in shape are difficult to inspect [86].

2.5. Thermography

Thermography is a contactless NDT technique, which can be used to inspect a specimen by using an infrared camera to provide thermal images of the specimen's surface temperature (see Fig. 17). There are two approaches to thermography: passive and active [90,91]. Passive thermography involves measuring the the spatial variation in temperature changes on the surface to reveal defects in the specimen. Passive thermography is used when the specimen is naturally at a different temperature to ambient. Active thermography involves the use an energy source to excite the specimen (e.g. a halogen lamp, ultrasound or eddy current sources) and the changes in temperature show the defects in the specimen. This is used to reduce the influence of the ambient environment and to give a greater contrast in temperatures to detect defects. The possible variations for setting up a thermography non-destructive test are presented in Fig. 18, where one element from each column is chosen to produce a complete system [90].

A local temperature increase seen in a specimen during a fretting fatigue test is related to the plastic deformation at the crack tip [127–129]. The work done at the crack tip is irreversible and most of this work done is given off as heat [128]. Thermography allows the detection and monitoring of crack initiation and growth through the detection of local temperature increases.

Recent works show the capability of using thermography in-situ with plain fretting [15] and fretting fatigue [92–95,130]. Berthel et al. [15] showed that thermography is a quick technique to use during a plain fretting loaded test in comparison to using a destructive method (one hour per experiment compared to one day per experiment, respectively) while being able to obtain similar results of the shear stress threshold (to cause crack nucleation) to within 10% of the destructive method values. Additionally, Chhith et al. [94,95,130] successfully performed fretting fatigue testing for a cylinder-on-flat geometry and elliptical contact and determined the number of cycles to crack initiation using in-situ thermography. Images were only recorded for the first 1000 cycles until a steady state for the partial slip regime was achieved, then coordinates for all the regions of interest were used as an input to a MATLAB script and the average temperature data was recorded throughout the test. An increase in the thermal elastic temperature amplitude from a predefined threshold was used to determine when crack initiation occurred. This was achieved for a minimum crack initiation size of 130 μm [94,130].

A limitation of using this technique is that the temperature rise needs to be high enough around the crack tip to be detected [131]. Also, environmental temperatures and heat conduction from the fretting fatigue device needs to be filtered in order to detect the temperature rise, as well as distinguishing other heat sources such as friction, plastic dissipation and thermal elasticity [94,130]. It should also be ensured that the specimen emissivity is not too low, where the specimen is reflecting the environmental temperature, therefore the surface of the specimen may need to be altered to improve the emissivity [90]. In addition, thermography only allows a limited thickness below the surface to be monitored, which can limit the results for complex geometries with larger thicknesses [90]; furthermore, the location of cracks can be difficult to obtain for complex geometries, as the camera cannot get a direct image around contacting surfaces. An improvement could involve using more than one infrared camera using triangulation to observe the 3D surface temperature of the specimen, which may pick up additional crack locations. An example includes combining the use of 3D scanners and infrared cameras to create a 3D thermal image of composite structures [132]. 3D scanners are used to form a reconstructed 3D model of the specimen and a method, such as using ray-tracing GPU rendering algorithms developed by Hellstein and Szwedo [132], is used to map the infrared images on to the 3D model.

2.6. Acoustic emission

Acoustic Emission (AE) involves the detection of transient elastic waves, produced from the mechanical vibrations within an elastic medium in the form of sound [133], from displacements within a specimen [66], created when energy is rapidly released from defects and cracks when a specimen is subject to a stress or load [99]. These waves are

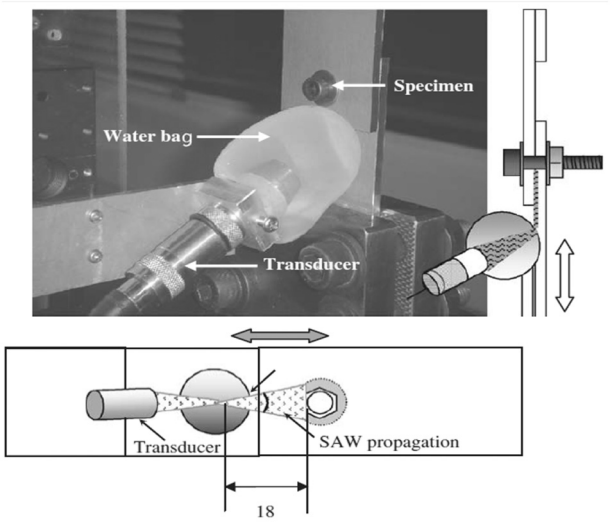

Fig. 16. Set-up for detecting fretting fatigue cracks using a water bag and surface acoustic waves (SAW) [10].

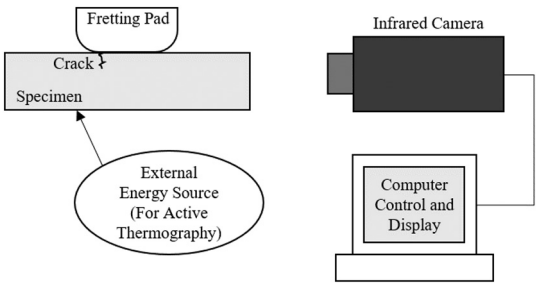

Fig. 17. Thermography method schematic.

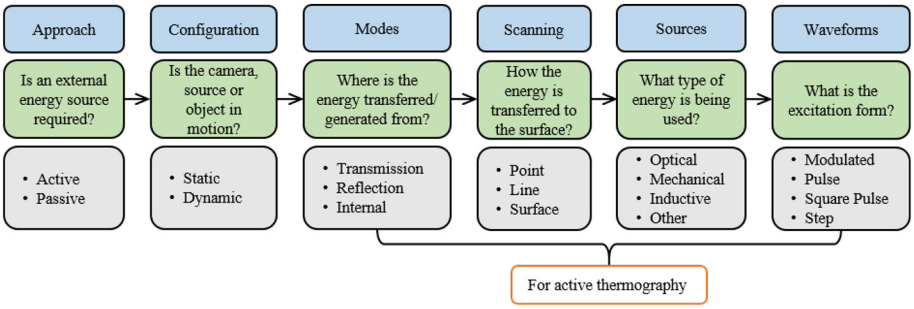

Fig. 18. Different elements used for designing a thermography NDT (Adapted from [90]).

received by a sensor placed on the specimen which converts the acoustic waves into electrical AE signals [66]. The signal is then picked up using acoustic emission detection equipment, which goes through signal processing and the waveform is displayed. The signal processing involves minimising background noise (e.g. that of the fretting contacts), identifying AE signal wave characteristics and showing when the AE signal exceeds an amplitude threshold, indicating the presence of a crack [66]. A schematic of the AE method is presented in Fig. 19.

AE has been used to detect cycles to crack nucleation and observe crack propagation in fretting fatigue [20,66,98–100] for a range of geometries including cylinder-on-flat [66], sphere-on-flat [98,99] and crossed cylindrical wires [20,100]. It has also been used in fretting wear experiments to determine the transition between slip regimes [134]. In addition, this technique has the capability of locating fretting fatigue cracks to be determined by using a locating method, such as delta-T mapping techniques [135,136] with plain fatigue tests, but has yet to be performed for fretting fatigue tests. With an AE in-situ with a cylinder-on-flat fretting fatigue experiment, it was found that three crack propagation modes could be identified [66]: mode II fretting cracking, mixed mode crack propagation and mode I pure fatigue cracking, as shown in Fig. 20. This also showed that the crack behaviour could be monitored with time. Another advantage of using AE, it has ability of detecting internal cracks and defects [137].

The main limitation of using this technique is that the AE signal produces a lot of scatter due to noise in the system (such as background noise and vibrations from the combination of the fretting loads and contact surfaces), which makes the signal difficult to interpret [20,66,98–100]; therefore, the user needs to be experienced in order to interpret the AE signals correctly. In addition, care has to be taken as the AE signal from different sources can overlap. Therefore, a technique has to be used to counteract this [66]. Meriaux et al. [66] used a real-time software known as Noesis®. This software splits the signals into groups, known as classes, which are determined by an Unsupervised Pattern Recognition (UPR) technique. UPR uses pattern recognition algorithms, which determine patterns within the data and groups them into classes. The user inputs a number of parameters, such as amplitude threshold and time, to direct the UPR technique; therefore, the quality of the results depends on on the user input of parameters.

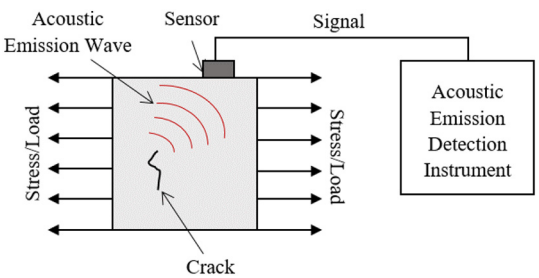

Fig. 19. Acoustic Emission method schematic.

2.7. Direct current potential drop

The potential drop (PD) technique involves the use of two probes to measure the voltage across the region of interest (as shown in Fig. 21), where a DC or an AC current (known as DCPD or ACPD, respectively) is passed through the circuit and a change in the crack length results in a change in the potential difference [62].

DCPD has been applied in-situ during many fretting fatigue tests [45,46,62,65,102–104,138,139] and has shown many benefits. Crack initiation can be detected with a minimum crack depth of 50 μm [65], which is highly sensitive in comparison to other techniques. Tests have been able to be performed for a high number of cycles in the order of 10^9 [103] and have proven the DCPD is capable of being used in a hydrogen gas environment [104,138,139]. Furthermore, the crack length can be calibrated with the PD results [62,65,102–104,138,139]. Meriaux et al. [65] used an empirical method, which involved monitoring the changes in the potential distribution around the crack with crack growth. The increase in electrical potential, V, was compared with the reference potential, V_0 (from the beginning of the test) and correlated to the average crack length. Tests were run to obtain different values of increased potential and interrupted for different average crack lengths. For small cracks (<600 μm), the test was interrupted at a chosen potential ratio value and the specimen crack length was measured optically. For cracks larger than these, the load ratio was varied from 0.01 to 0.5 and from 0.5 to 0.01. The crack length was then determined from optical measurements. The calibration process was then repeated to confirm the results. With this data set, a polynomial function was used to correlate the potential and the crack length. Fig. 22 shows the top two plots as the potential ratio, V/V_0, against the number of cycles in a fretting fatigue test for a peak bulk stress, σ_{fat} of 350 MPa and 400 MPa. The bottom two plots show the corresponding crack evolution the crack length (μm) over the sample depth (mm), a/W, against cycles, found from a fitted calibration curve from the potential drop results. Each curve in the plot represents a different tangential load divided by its normal load (Q/P ratio). The number of cycles to crack initiation was found from these plots as well as the modes of crack propagation. The cycles to crack initiation was defined as the start of the curve from the lower plots in Fig. 22. This is where the minimum crack depth was detected at 50 μm. Each curve presents the same shape, which can be linked to the different modes of crack propagation from the change in slope of the curves. The change in slope appears at crack lengths between $a/W = 0.015$ and $a/W = 0.025$. Below this point corresponds to mode II and mixed mode crack propagation, while above this point corresponds to mode I propagation. The number of cycles to crack arrest and failure have also been obtained from the potential slopes [45,62,65,102].

The limitation to using this technique is that the approximate location of the crack needs to be known, which can be difficult for complex and large geometries. In addition, by not knowing the location of the crack and the direction of crack growth, it is not possible to gain a representation of the crack path and shape. Furthermore, the technique is

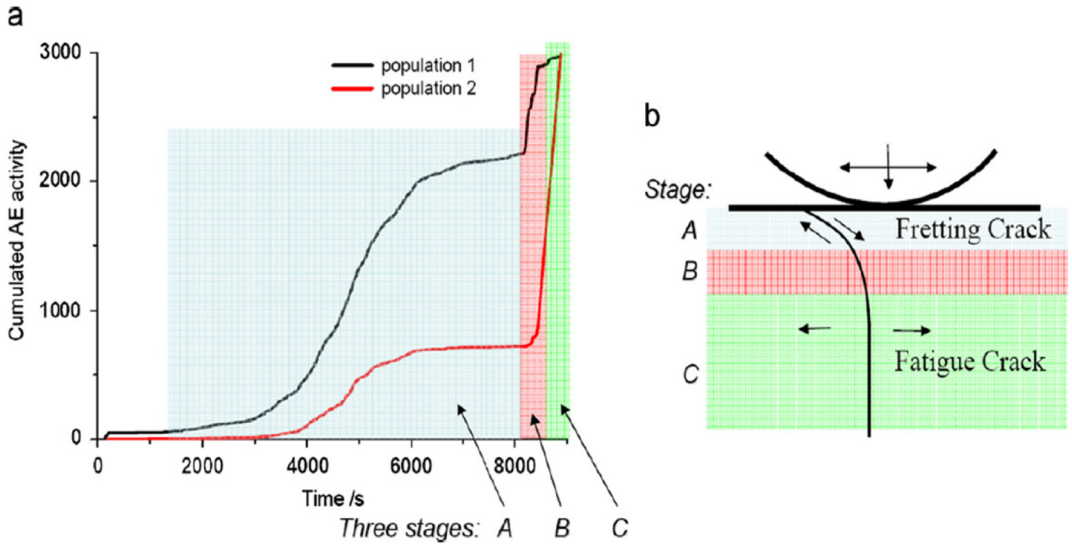

Fig. 20. Results from an AE in-situ with a cylinder-on-flat fretting fatigue experiment. a) shows the three stages of crack propagation identified from the cumulated AE activity and b) shows the representation of the crack stages [66].

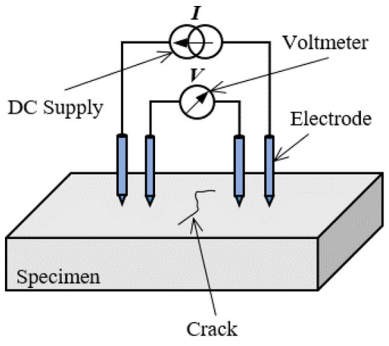

Fig. 21. Potential drop method schematic.

not contactless, as the wires have to be welded onto the specimen [62], which can have an affect on the surrounding microstructure. Special care needs to be taken to limit scatter and reduce noise, therefore positioning of the wire probes becomes important and needs to be optimised, where the approximate area of crack initiation is known so that a crack can be initiated between the probes [62,65]. The quality of detection becomes less efficient if a crack is produced on a different face to where the the probes are attached and therefore, a correction of the reference potential is needed to take this into account [65]. Also, the need for a calibration curve for each type of load is required and this is currently dependent on repeat tests using the destructive method [65]. This is not efficient if multiple loading conditions need to be carried out and could become expensive.

3. Comparison of techniques

3.1. Sensitivity

The minimum crack length that can be detected using a technique is analogous to crack sensitivity, allowing these to be compared across NDT techniques in-situ with fretting fatigue tests. Fig. 23 displays a bar chart of the minimum crack depth detected for crack initiation from the different NDT techniques used for fretting fatigue experiments. The lower the minimum crack depth detected, the higher the sensitivity the NDT technique is. These techniques can be split into imaging frequency dependent techniques and techniques dependent on the signal response detection.

Imaging frequency dependent techniques include replica optical microscopy (ROM), video microscopy (VM), scanning electron microscopy (SEM) and X-ray radiography (XR). The bar chart shows that SEM has the highest sensitivity with a minimum crack length detected of less than 1 μm [77]. Han et al. [77] found this from an initiation of a secondary crack during a fretting fatigue test, where as the primary initiation crack length was approximately 17.3 μm. It was found that using this technique, the crack length for crack initiation varied from test to test and with the imaging frequency was not being published. Therefore, it is difficult to completely conclude how sensitive this technique is, as the minimum length of the crack detected will depend on the frequency on the images being taken. The next sensitive imaging frequency dependent technique was VM with a minimum crack length detected of 40 μm [70,71]. Compared with XR and ROP, a higher imaging frequency was used, interrupting tests every 200 cycles until a crack was found and therefore was able to pick up smaller cracks. XR used in-situ with fretting fatigue tests was able to detect a minimum crack depth of 100 μm [85]. This technique relied on the frequency of the radiographic images being taken every 5000 cycles. ROP showed to be the least sensitive with a minimum crack detection of 200 μm [73]. This was due to how much detail the replica could pick up of the crack, as well as the frequency of imaging taking place. To improve the sensitivity of any of these imaging techniques, tests require a higher image frequency until a crack is found. It should be advised to do an initial test to determine optimum imaging frequency. Overall, it can be seen that in Fig. 9 the resolution and magnification is higher using SEM compared with VM and XR images shown in Figs. 6 and 12, respectively. Therefore, SEM can pick up on more information and smaller details; however, to make a complete conclusion of the sensitivity between imaging frequency dependent methods, tests need to be carried out where the imaging frequency is the same for all methods for the same testing conditions.

For the signal dependent techniques, it can be seen from Fig. 23 that acoustic emission is the most sensitive technique with the ability of detecting crack initiation, by an increase in the cumulative AE energy at a length of less than 8 μm [66]. The crack length was determined by destructive testing and measuring the crack length using SEM. It is known from previous plain fatigue tests that AE is more sensitive than ultrasound techniques, as AE was able to detect a crack earlier [140]. To confirm these results without using a destructive method, it is possible to combine AE with OM or SEM to determine the length of crack initiation detected by AE. In-situ AE with

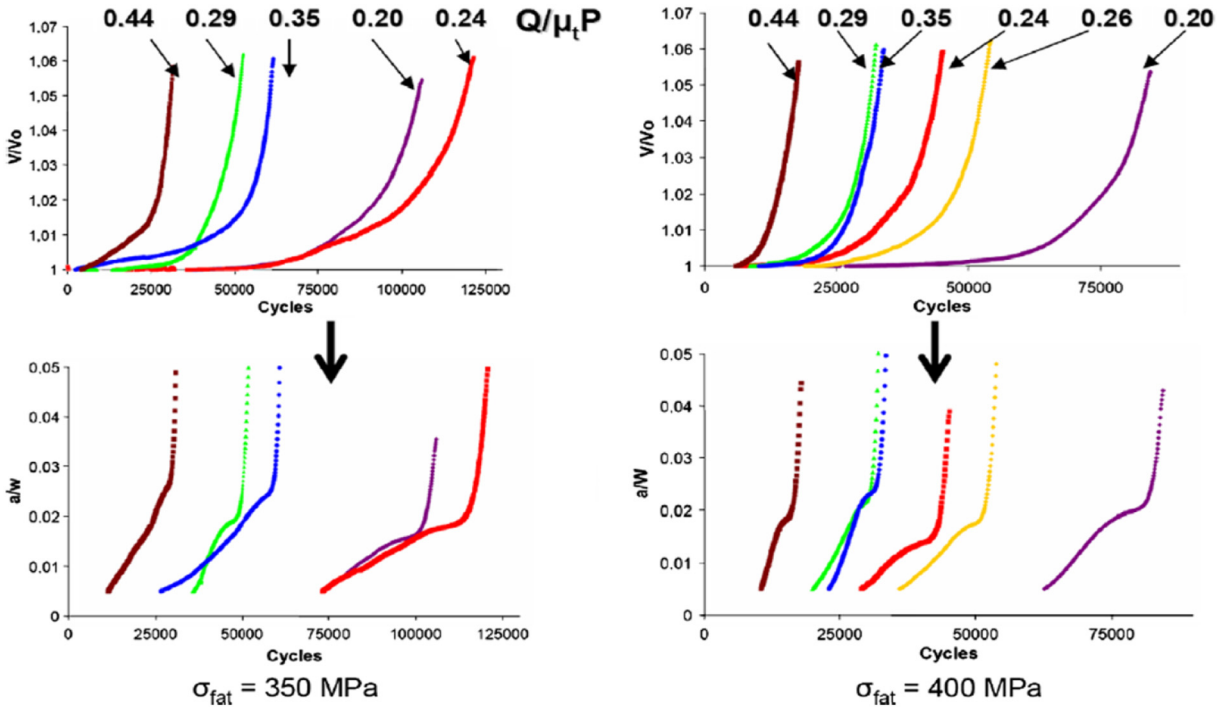

Fig. 22. Results from using the PD technique. Top two plots present V/V_0 against the number of cycles ($\sigma = 350$ MPa and 400 MPa, respectively) and the bottom two plots are the calibrated results of a/W against the number of cycles [65].

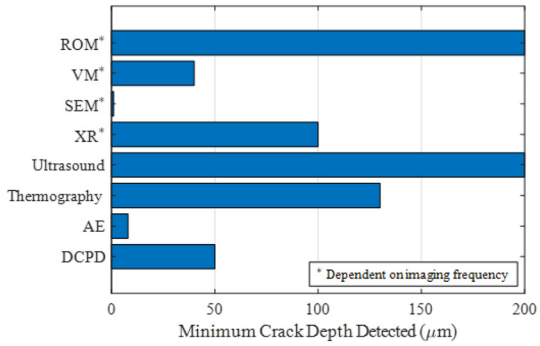

Fig. 23. Comparison of the sensitivity of NDT techniques used during fretting fatigue experiments (data from [10,37,65,70,73,74,77,85,87,94]).

OM or SEM for plain fatigue tests have been carried out before to distinguish AE signals [119] and monitor crack length [97]. In addition to confirming the differences in AE signals. The next most sensitive technique was found to be the direct current potential drop (DCPD) technique with a minimum crack length detected of 50 μm [65] by an increase in the electrical potential with respect to its reference value; however, it has been stated by Kondo et al. [103] that DCPD was capable of detecting crack lengths of a few tens of microns, but an actual value was not specified. The approximate location of crack initiation needs to be known to use this method, if the estimated location is more accurate, the sensitivity is higher. The DCPD technique sensitivity may be improved further by using ACPD, due to the skin effect [101,103]. For thermography, Chhith et al. [94] detected a minimum crack size of 130 μm during a fretting fatigue test by a deviation of the thermo-elastic amplitude from its stabilised pre-crack value. The minimum achievable pixel size of the thermal images for this test was 65 μm and therefore, this crack size corresponds to two pixels. To improve the sensitivity of this technique, it has been suggested that an upgraded infrared image sensor with a smaller thermal image pixel size and higher pixel density could be used to detect smaller cracks [94]. This could, also, improve the measurement of crack lengths, which can be monitored from thermal images, as suggested with an in-situ fatigue test by Urbanek and Bär [141]. The least sensitive out of the signal dependent techniques was found to be the ultrasound technique (using the water bag technique [10] and the shear wave technique [87]) with a minimum crack depth of 200μm. To improve the sensitivity of the ultrasound technique, the ultrasound signal can be designed to focus on areas where smaller cracks are expected to appear [88]. Furthermore, laser ultrasound may be a chosen alternative as it has been claimed to have higher sensitivity than traditional ultrasound techniques [142].

A comparison of the minimum crack length that can be detected by the different techniques is an important consideration with respect to the microstructure of the material being investigated. The mechanics approach to crack initiation classes crack initiation as the formation of a crack of the order of a few grain sizes or less. This means that when choosing a technique, it should be ensured that the technique is capable of capturing a crack initiation length in the order of grain sizes of the material being used, meaning a material with finer grain sizes will require a more sensitive technique. Only by choosing the appropriate technique will data be available concerning crack initiation size, crack orientation and initial crack propagation be available for lifing approaches and validation of micro-mechanics modelling approaches. Overall, Fig. 23 displays a graphical comparison of the sensitivity of the NDT techniques used in-situ during fretting fatigue experiments from the available literature. All techniques were able to detect cracks less than 200 μm. The sensitivity of each technique relies on the resolution of the equipment, how the method is used and the user's experience with the technique and equipment [17]. Particularly for imaging frequency dependent techniques, the frequency of images taken during the early stages of tests to determine cycles to crack initiation should be optimised.

3.2. Number of cycles to crack initiation

The total lifetime of a component is the summation of the number of cycles to crack initiation and the number of cycles of crack propagation before failure. Improving the understanding of these phases can aid design against crack initiation and prolong crack propagation to increase the lifetime of components by comparing different testing parameters, such as geometry, loading, material etc. These can also be used to aid and validate modelling methods to improve the understanding of fretting fatigue and prevent premature failure of components. The NDT techniques used in-situ with fretting fatigue tests for determining the number of cycles to crack initiation are compared with respect to how the point of initiation is determined, the available data within the literature and the reliability of each method.

For imaging based methods (such as OM, SEM and XR), the number of cycles to crack initiation is determined by interrupting the test at a specified number of cycle intervals and an image is taken until a crack is visible in an image. For ROM, Majzoobi et al. [73,105–107] performed many fretting fatigue tests for various peak bulk stresses with no tangential loading for various surface modifications and coatings, where tests were interrupted every 5000 cycles. The number of cycles to crack initiation with respect to peak bulk stress is shown in Fig. 24. It can be seen that specimens with shot peening and a test frequency of 5 Hz follows a similar trend to that with a test frequency of 20 Hz, with initiation life reduces as expected; however, both results deviate from the general trend from other specimens that as the peak bulk stress increases, the crack initiation lifetime reduces. This may be explained the variation of crack initiation size between tests. This is believed to be due to the imaging frequency not being high enough. Abbasi et al. [37,108] and Majzoobi et al. [74] performed similar experiments, but using a cyclic normal load instead of a constant normal load and tests were interrupted every 1000 cycles. Cycles to crack initiation results are shown in Fig. 25 with respect to temperature for a bulk stress of 130 MPa and in phase loading between normal load and bulk load for unmodified specimens and a specimen with shot peening, as well as unmodified specimens for out of phase loading. It can be seen that there was a repeat test for specimens with no modification at room temperature (assumed to be 20 °C), where the percentage difference between initiation lifetime was found to be 7.7%. In Fig. 26, a comparison between the crack initiation length for all the tests and its corresponding peak bulk stress (above each bar) that were interrupted every 5000 cycles in comparison with tests that were interrupted every 1000 cycles. It can be seen that there was much more variation in the crack length for tests interrupted every 5000 cycles, where lengths ranged between approximately 0.2 mm to 2.2 mm; whereas tests that were interrupted every 1000 cycles proved to be more consistent with an average crack initiation length of 260 μm. This shows that by increasing the imaging frequency, a more consistent crack initiation length can be found and therefore, crack initiation lifetime results become more consistent and reliable.

Moreover, results using VM are summarised in Fig. 27, where repeat tests where done under the same loading conditions and parameters by two separate works [70,71], where tests were interrupted every 200 cycles. Arora et al. [70] performed three repeat tests for each combination of Q/P and peak bulk stress and plots of cycles were presented with crack size, which proved to be consistent between test. However, determining the cycles to crack initiation for each repeat test was difficult due to overlapping data and the use of the same marker symbols on plots, so the data presented in Fig. 27 by Arora et al. show the shortest cycles to crack initiation that could be found from crack growth plots. This may contribute to any errors between the two sets of results. It can be seen that the repeat tests at peak bulk stress of 300 MPa and 325 MPa are more consistent and follow the same trend with an average percentage difference of 26% and 6.5%, respectively, whereas tests that were performed at 290 MPa show different trends with an average percentage difference of 54%. This shows it is vital to have repeat tests and ensure

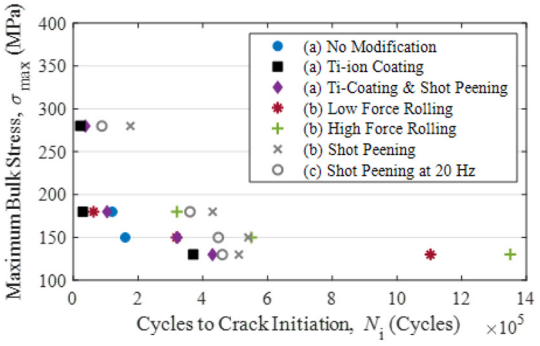

Fig. 24. Number of cycles to crack initiations using replica optical micrography varying with σmax for specimens with various surface modifications and/or coatings (data from (a) [106,107], (b) [73] and (c) [105], where a micrograph taken of replica every 5000 cycles until crack observed. Parameters of the tests include: Al-7075-T6 specimen, stainless steel 410 flat pads, $P = 1200$ N, $f = 5$ Hz (unless specified) and R-ratio=0.1.).

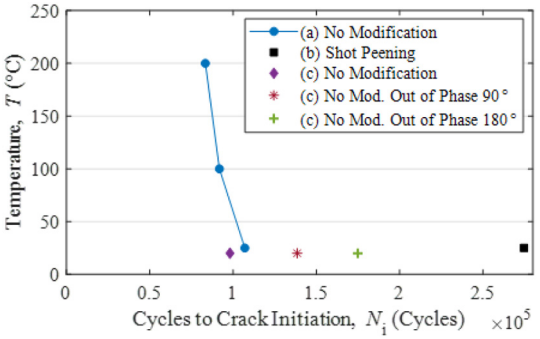

Fig. 25. Number of cycles to crack initiations using replica optical micrography varying with (a) temperature for no surface modification data from [37] and at room temperature for (b) a specimen with shot peening [74] and (c) a unmodified specimen for in phase loading for normal and bulk loads and out of phase loading [37] (A micrograph taken of replica every 1000 cycles until crack observed. Parameters of the tests include: Al-7075-T6 specimen, stainless steel 410 flat pads, $P_{max} = 1200$ N (using a cyclic normal load), $f = 10$ Hz, σmax=130 MPa and R-ratio=0.0.)

there are no other contributing factors contributing towards any errors. Also, it should be noted that ROM tests that were interrupted every 1000 cycles [37,74,108] used modelling methods to determine the crack initiation length (which is in the order of a few grains of a material), where linear elastic fracture mechanics can be used. It was found the modelled crack initiation length was 50 μm, which was less than the 260 μm detected by ROM, so modelling methods were used to predict the cycles to initiation at 50 μm based on experimental crack growth data. In comparison, authors using VM [70,71], who used the same specimen material, did not need to predict cycles to crack initiation as the crack initiation length detected was in the range of 40 μm to 60 μm and instead used separate modelling methods to compare with experimental results [71].

Table 2 shows all the available data from the literature for cycles to crack initiation, which cannot be presented in plots. Variables in the table include the material of the specimen, material of the pad, radius of the cylinder (or sphere), R, the tangential load and normal load ratio, Q/P, the stress R-ratio, the load frequency, f, the peak bulk stress, σmax and the number of cycles to crack initiation, N_i.

Results for SEM shows a limited data set found from three tests, where the frequency of the images being taken was not published, so it is difficult to compare N_i confidently. The method was able to achieve results for tests with temperatures of 400 °C. It was found that using this technique, the crack initiation length varied from test to test, which may suggest the imaging frequency was different between tests or there was not a consistent method of determining when crack initiation occurs. This may be due to the authors being primarily interested in the

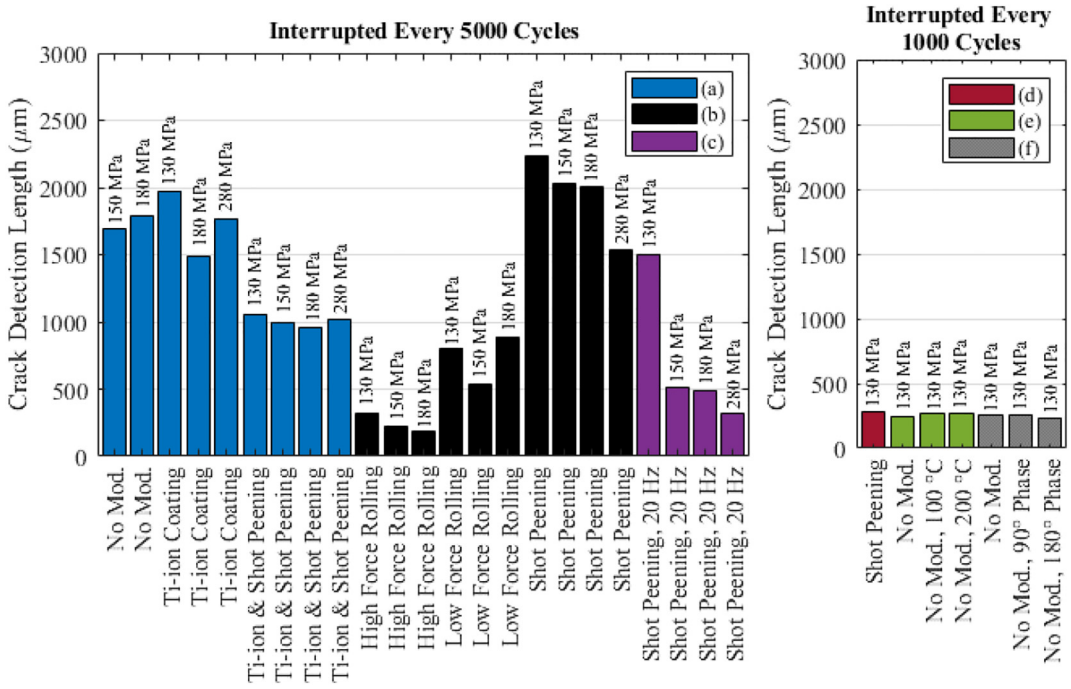

Fig. 26. A comparison for crack initiation length for ROM tests interrupted every 5000 cycles from datasets (a) [106,107], (b) [73] and (c) [105] (Al-7075-T6 specimen, stainless steel 410 flat pads, $P = 1200$ N, $f = 5$ Hz (unless stated otherwise) and R-ratio=0.1) with ROM tests interrupted every 1000 cycles from datasets (d) [74], (e) [37] and (f) [108] (Al-7075-T6 specimen, stainless steel 410 flat pads, $P = 1200$ N, $f = 10$ Hz, σmax=130 MPa and R-ratio=0.0).

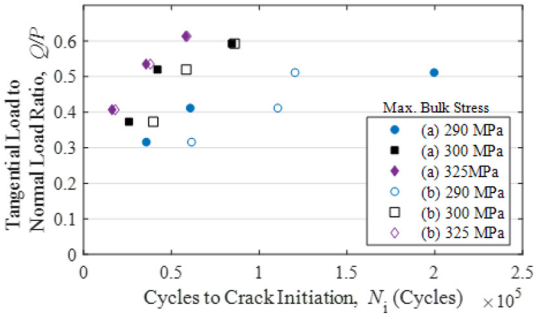

Fig. 27. Number of cycles to crack initiations using video micrography varying with Q/P and σmax (data from (a) [70] and (b) [71]), where the Region was scanned every 200 cycles using an optical microscope until crack observed. Parameters of the test include Al-7075-T6 specimen, En24 steel flat pads, $f = 10$ Hz and R-ratio=0.1).

evolution of initial crack propagation and its microstructure; although, determining when crack initiation occurs at an early stage is a contributing factor that should be taken into account to observe how a crack initially propagates.

Results for XR show two cases found in 3, which show an approximation of N_i. Proudhon et al. [120] took a radiograph at 50×10^3 cycles (based on previous works that determined the loading to initiate a fretting fatigue crack [143]) to show crack initiation, which gave a crack initiation length of 100 μm. DePannemaecker et al. [85], under different test conditions, could not rely on previous works and therefore obtained the cycles to initiation by interrupting the test every 5000 cycles until a crack was observed. The value of the number of cycles published was an approximation and had a tolerance of −5000 fretting cycles and hence, this technique relies upon how often the tests are interrupted like other imaging based methods.

Data for N_i from using the ultrasound technique using shear wave inspection [87] is presented in Table 2. The authors did three repeat tests for these loading conditions, where one test was not reported as the crack went undetected. Ultrasound signals were compared every 500,000 cycles due to the high frequency of 300 Hz until changes in the amplitude and shape of the ultrasound wave was found. The repeat tests show that one was unsuccessful and there was 13.6 % difference between the other two tests for crack initiation lifetime. In addition, the authors found that at a lower normal stress of 200 MPa, cracks went undetected [87] and therefore, this technique was not reliable for lower normal stresses. Advancements in monitoring fatigue cracks with ultrasound may improve the practicality and reliability of these results.

Thermography results for N_i are presented in Table 2 for cylinder-on-flat and elliptical contact geometries [94,130]. N_i was determined by a deviation in the thermo-elastic amplitude from its stabilised value. For two repeat tests under the cylinder-on-flat geometry show a percentage difference in N_i of 49 %, whereas for the elliptical contact geometry two repeat tests showed a percentage difference of 16 %. Further repeat testing should be performed to understand the variability between tests to ensure it is not the method causing the differences and that its other factors are causing these. It was also found that the crack initiation length ranged between 208 μm and 580 μm for elliptical contact, while for the cylinder-on-flat contact crack initiation length ranged between 130 μm and 220 μm. This shows that changing geometry may change the method's ability in detecting a consistent crack initiation length.

Results for AE are presenting in Table 2, where only two cases were reported N_i for a sphere-on-flat geometry [98,99]. It was also found that for cylinder-on-flat experiments, it was possible to obtain the time to crack initiation [66], but the cycles to crack initiation were not reported. Authors seemed to be primarily interested in the crack propagation stage, giving the limited data set. Due to no repeat tests it is not possible to conclude the reliability of detecting cracks consistently, which will be depend on the filtration method used. It also needs to be confirmed using image based method in-situ with AE to obtain crack initiation size to understand the consistency between results.

DCPD results by Meriaux et al. [65] for cylinder-on-flat fretting fatigue tests are summarised in Fig. 28. A crack was detected when there was an increase in the electric potential from its reference

Table 2
Cycles to crack initiation for a cylinder on flat fretting fatigue tests with various parameters determined by various NDT techniques.

NDT Technique	Determination of Crack Initiation	Material of Specimen	Material of Pad	R (mm)	Q/P	f (Hz)	σmax (MPa)	R-Ratio	N_i (Cycles)
SEM [77]	Test was paused and scanned using SEM until crack observed	NBSX - Orientation A	NBSX	0.75	367.4[e]	10	98	0.1	189,934
SEM [76]	Test was paused and scanned using SEM until crack observed	NBSX - Orientation A at 400◦C	NBSX	0.75	426[e]	10	98	0.1	175,342
SEM [76]	Test was paused and scanned using SEM until crack observed	NBSX - Orientation B at 400◦C	NBSX	0.75	426[e]	10	98	0.1	67,014
XR [120]	A radiograph was taken at 50×10^3 cycles based on previous literature [143].	Al-2024	Al-7075-T6	49	0.75	20	100	0.2	50,000
XR [85]	A radiograph was taken every 5000 cycles until a crack is observed.	Al-7050-T741	52,100 Steel	10	0.78	12	167.5	0.29	30,000
Ultrasound [87]	Changes in amplitude and shape of reflected ultrasound wave.	Ti-6Al-4 V	Ti-6Al-4 V[c]	—	0.10	300	260	0.5	7,019,649
Ultrasound [87]	Changes in amplitude and shape of reflected ultrasound wave.	Ti-6Al-4 V	Ti-6Al-4 V[c]	—	0.10	300	260	0.5	6,125,123
Thermography [94,130]	A deviation of the thermo-elastic amplitude from the stabilised value	Al-2024-T3	Al-2024-T3	50	0.61	5	200	0.001	42,962
Thermography [94,130]	A deviation of the thermo-elastic amplitude from the stabilised value	Al-2024-T3	Al-2024-T3	50	0.61	5	200	0.001	66,134
Thermography [94,130]	A deviation of the thermo-elastic amplitude from the stabilised value	Al-2024-T3	Al-2024-T3	50	0.59	5	187.5	0.001	70,044
Thermography [94,130]	A deviation of the thermo-elastic amplitude from the stabilised value	S235JRC Steel	S235JRC Steel	150	0.71	5	440	0.001	58,548
Thermography [94,130]	A deviation of the thermo-elastic amplitude from the stabilised value	S235JRC Steel	S235JRC Steel	150	0.60	5	400	0.001	80,075
Thermography [130]	A deviation of the thermo-elastic amplitude from the stabilised value	Al-2024-T3511	Al-2024-T3	200/27.5[b]	0.24	5	220	0.001	46,580
Thermography [130]	A deviation of the thermo-elastic amplitude from the stabilised value	Al-2024-T3511	Al-2024-T3	200/27.5[b]	0.24	5	220	0.001	54,702
Thermography [130]	A deviation of the thermo-elastic amplitude from the stabilised value	Al-2024-T3511	Al-2024-T3	200/27.5[b]	0.22	5	200	0.001	110,975
Thermography [130]	A deviation of the thermo-elastic amplitude from the stabilised value	Al-2024-T3511	Al-2024-T3	200/27.5[b]	0.22	5	180	0.001	135,515
AE [99]	An increase in the acoustic event rate	Ti — 17	Ti-6Al-4 V[a]	400	0.46	10	750[d]	0.10	125,000
AE [98]	An increase in the acoustic event rate	Ti — 17	Ti-6Al-4 V[a]	400	0.46	10	360	0.10	70,000
DCPD [102]	An increase in the electrical potential from the reference value	32Cr1 Steel	FM35 Steel	4.6	0.30	12	$0.78\sigma_{y,f}$	0.85	100,000
DCPD [138,139]	An increase in the electrical potential from the reference value	SCM435H Steel	SCM435H Steel[c]	–	0.20	18.7	170[f]	−1	53,961
DCPD [138,139]	An increase in the electrical potential from the reference value	SCM435H Steel in H	SCM435H Steel in H[c]	–	0.20	18.7	170[f]	−1	574,893
DCPD [104]	An increase in the electrical potential from the reference value	Pre-Strained SUS304 Steel	Pre-Strained SUS304 Steel[c]	–	0.43	18.7	160[f]	-1	5,087,045
DCPD [104]	An increase in the electrical potential from the reference value	Pre-Strained SUS304 Steel in H	Pre-Strained SUS304 in H Steel[c]	–	0.52	18.7	160[f]	-1	1,014,298

[a] Spherical pad.
[b] Elliptical contact (Radius of pad/Radius of specimen).
[c] Flat pad.
[d] Constant.
[e] Contact force (N) - No tangential force.
[f] Nominal stress amplitude (MPa) for bending fretting fatigue test.

potential value. Results by Meriaux et al. [65] for cylinder-on-flat fretting fatigue tests are summarised in Fig. 28. It can be seen that there are a few discrepancies, such as N_i for a Q/P of 0.24 and 0.2 and a σmax of 350 MPa are the same. This is due to difficulty in distinguishing N_i between the two crack curves as these were overlapping in Fig. 22. It can be seen that by increasing σmax to 400 MPa, there is a fluctuation in the number of cycles to crack initiation. The authors suggested this was the effect of increasing the bulk load, but it should also be mentioned that calibrations curves need investigating more with respect to each testing condition. A suggestion may involve in-situ OM or SEM instead of the destructive method with repeat testing to obtain the calibration curves to ensure reliability of the method. Other DCPD results available in the literature is presented in Table 2, which show results for another cylinder-on-flat test [102] and results for a bending fretting fatigue test under air and hydrogen environments [104,138,139]. This shows that this method is capable of being applied to other types of fretting fatigue testing and can measure crack growth under alternative environments. It was found with all the results obtained from using DCPD that the works were primarily interested in crack growth rather than initiation. Future work should also focus on crack initiation, as this method can detect cracks without the need for interrupting the test.

Overall, this analysis shows the limited amount of data available for research in this area. It is difficult to draw conclusions of the number of cycles to crack initiation for fretting fatigue tests, especially for various pad geometries and testing methods. This shows that a larger database needs to be collected in order to draw conclusions regarding the conditions that lead to crack initiation for a set of given test parameters. Tests with the same loading variables and parameters need to be carried out across the available NDT techniques to give a unified comparison of the applicability of these techniques for collecting this data. It can be seen that there are many influential factors that affect the cycles to crack initiation and the effect of each parameter needs to be isolated. In addition, repeated testing is essential to prove the reliability of all these methods. Furthermore, imaging based techniques need to optimise the imaging frequency to ensure consistency and reliability of the results. Signal techniques are useful in identifying crack initiation without interrupting

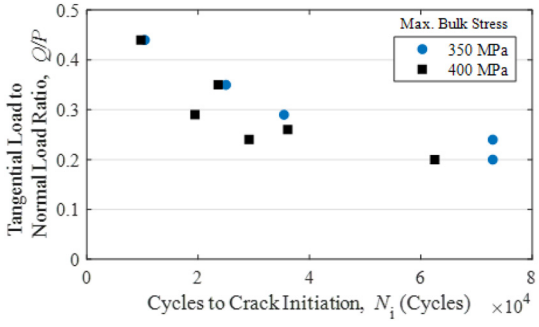

Fig. 28. Number of cycles to crack initiations using direct current potential drop method varying with Q/P and σmax (data from [65]) (Ti-6Al-4 V specimen, Ti-6Al-4 V cylindrical pad, $R = 40$ mm and $f = 10$ Hz. An increase in the electrical potential from the reference value).

tests, but reliability of some techniques are uncertain. A suggestion to improve this could involve initially using imaging based methods in-situ with signal techniques to validate or complement the method.

3.3. Capability of techniques

A comparison of the NDT techniques for inspecting fretting fatigue cracks is presented in Table 3. All the capabilities are the main outputs that are required for inspecting fretting fatigue cracks with in-situ NDT, as listed in the introduction. It was noted that all techniques were either unable or not have been done yet to monitor the crack shape due to the lack of 3D crack monitoring. This is particularly important if cracks are not through cracks through the thickness of the specimen, there are multiple initiation sites and for various geometries, such as spherical-on-flat [98,99], which had ellipsoid crack shapes. Crack shapes are usually analysed through post-mortem examinations and little is known about how crack shapes evolve.

It was found that OM, SEM and XR are most successful in satisfying all conditions. Due to these being imaging techniques, the images obtained from these experiments are ideal for identifying the crack locations, crack growth length, crack propagation modes and crack growth path; however, it should be noted that there is a tolerance to which the user can identify the number of cycles to crack initiation is dependent on the frequency the fretting fatigue test is interrupted to scan and take these images. This involves the user being proactive in finding the crack initiation. Possible future suggestions to automate this may include combining machine learning models such as neural networks to determine whether a crack has been detected or not. The main benefit XR has from the other two methods is that it can detect internal cracks. This means there is scope to improve the XR method, it would be ideal if 3D rendered images could be found for the cracks using X-ray computed tomography in-situ with a fretting fatigue test to obtain a 3D evolution of fretting fatigue cracks [85]. Furthermore, it is worth noting that SEM has a great advantage over other methods in determining the effects of microstructural features, such as slip lines and inclusions, which may contribute to the initiation of cracks and the evolution of cracks. This method is ideal for exploring the microstructural mechanisms that contribute to fretting fatigue cracks.

Ultrasound could be potentially the next most promising technique. It has not yet been used to investigate the crack propagation during a fretting fatigue test. It has the potential to improve its capability from recent works of using ultrasound for other applications. Further research suggestions includes further investigation into the feasibility of the laser ultrasound technique [142,144] or the feasibility with the use of ultrasound transducer arrays with imaging methods to detect cracks [145]. This will allow the detection of crack location and data for crack propagation. Ultrasound has not yet been able to identify crack propagation modes. However, the specimen could be utilised after the test has finished by the use of a destructive method, where the propagation modes could be identified.

Thermography is the next most promising technique. This technique has been used in-situ with a fretting fatigue test to investigate crack initiation, but has yet to be used to investigate crack propagation during a fretting fatigue test. Therefore, from the thermography images, it has been possible to obtain visual images of cracks initiating and has given data on the number of cycles to crack initiation and the crack location. This technique has the potential to monitor the crack length and crack path, but has yet not been able to identify crack propagation modes. Further work should involve using thermography to investigate the crack propagation during a fretting fatigue test. Furthermore, work should, also, involve upgrading infrared image sensors to detect smaller cracks. If the technology advances, it could be possible to obtain images of the crack shape. In addition, by using multiple infrared cameras, it could be used to observe the crack path and shape in three dimensions, which may have not been captured otherwise. Moreover, it could be possible to couple up with a destructive method to obtain data on crack propagation modes and crack shape, such as Vazques et al. [24] using the destructive method and a confocal microscope.

The AE technique has limitations for monitoring the crack growth length, crack growth path and shape. Suggested future work could involve calibrating the AE signals with the crack length and coupling up with either OM or SEM NDT techniques, such as those for plain fatigue test [97,119], or destructive methods, such as Meriaux et al. [65] using with SEM to calibrate potential drop measurements, to obtain a relationship. Furthermore, Meriaux et al. [66] suggested that AE could also be coupled up with potential drop techniques. This would be feasible, if the user only wanted additional data for the crack growth length. This could be made possible by locating the crack using AE and monitoring crack propagation from potential drop techniques. The difficulties with this is the implementation of both techniques with the fretting fatigue test rig would not be trivial and this would require a potential drop crack growth calibration for test under particular loading conditions and parameters regardless.

DCPD is a sensitive technique, but the location of the crack needs to be known and it cannot monitor the crack path and shape. This will be difficult to use in complex structures, where multiple crack initiation sites may occur. A suggestion could be that this technique could be coupled up with SEM or OM to find the location of the cracks, which can also be used to help with the improvement of crack length calibration for potential drop results instead of using destructive methods.

Other capabilities that should be included to improve the understanding and knowledge of fretting fatigue is the capability of monitoring microstructure throughout the tests. This is important to gain understanding on the fundamentals of fretting fatigue as the material microstructure influences the crack initiation process and how a crack propagates. This can aid design to prevent fretting fatigue cracks by making alterations to the microstructure of the material, such as surface modifications and heat treatments, and support modelling methods to prevent crack initiation and slow down crack propagation. Monitoring the microstructure could provide improved understanding on how cracks initiate and how a crack initiatially propagates for different materials and geometries. There has been little research in this area with regards to fretting fatigue and has only been investigated by using SEM for single crystal nickel-based superalloys [76–80], where the evolution of crystallographic slip and dislocation distributions have been observed with respect to the evolution of a fretting fatigue crack, which were used to validate a crystal plasticity finite element method. Furthermore, surface damage at an asperity level can be investigated and information on how this influences crack initiation [18]. This has also been applied to SEM with fretting fatigue testing to assess the surface damage and delamination of plasma-sprayed hydroxyapatite coatings [116].

Overall, SEM is the most suitable for gaining the most information from a fretting fatigue test based on the capability comparison table

Table 3
Comparison of the capabilities of several NDT techniques for fretting fatigue testing. A tick (✓) = the conditions is satisfied, a cross (✘) = the condition is unsatisfied and a tilde (~) = the condition has not yet been done.

NDT Technique	Cycles to Crack Initiation?	Monitor Crack Growth Length?	Identify Crack Propagation Modes?	Monitor Crack Growth Path?	Monitor Crack Shape?	Detect Crack Location?
OM	✓[a]	✓	✓	✓	✘	✓
SEM	✓[a]	✓	✓	✓	✘	✓
XR	✓[a]	✓	✓	✓	✓	✓
Ultrasound	✓	~	✘	~	~	~
Thermography	✓	~	~	~	✘	✓
AE	✓	~	✓	✘	✘	✓
DCPD	✓	✓	✓	✘	✘	✘

[a] Dependent on imaging frequency.

and the microstructural evolution evaluation ability; however, every technique is subjected to its own limitations and other advantages. Selecting the most suitable technique will depend on the result the user wishes to achieve, such as one may be primarily interested in monitoring crack growth, and the practical aspects of achieving these results. General practical aspects to consider include noise due to the contact and loading effecting the quality of crack detection, techniques that require limited space, techniques that need a visible field of view and techniques that require an approximate location of the crack. In addition, there is scope for future research to improving the capabilities on what can be achieved for in-situ fretting fatigue testing with each of the NDT techniques reviewed. Challenges include being able to collect a database from NDT techniques for in-situ fretting fatigue tests with the same test conditions and parameters, in order to reach a complete conclusion of the comparison of techniques.

3.4. Design implications

The main purpose of fretting fatigue tests is to design against failure by improving lifing of components through materials characterisation testing and component testing. The tests characterise the fretting fatigue behaviour of the material and contact conditions, which can be used to improve the understanding and design of components. The main outputs from these tests include the fundamental understanding of fretting fatigue cracks and obtaining lives of a component including crack initiation and crack propagation lives with respect to loading and contact conditions. The efficiency of methods to monitor fretting fatigue cracks is important with regards to design. Fretting fatigue tests include many cycles, many tests under different testing parameters and repeat tests to confirm the reliability of the results. To monitor crack growth using destructive techniques, many fretting fatigue tests are run for various number of cycles. For each test the crack length is measured using a destructive technique, which is then related to the number of cycles the test was stopped at [65,66]. This means many specimens are used and therefore, repeatability using this method is inefficient as it leads to wastage of material and time. Therefore, NDT techniques are ideal for monitoring cracks from fretting fatigue tests, as these methods allows the user to characterise crack growth rates/regimes more efficiently and can be used to develop new models and approaches to lifing that can be applied to design and lifing of components. Furthermore, these methods provide a richness of additional data, which may include identifying the time of crack initiation, monitoring crack growth, crack paths, crack orientation and crack shape, as well as identifying modes of crack propagation. From this, it is possible to validate modelling approaches for fretting fatigue crack initiation and growth predictions (e.g. SWT parameter, MTS criterion, etc.), which can be applied to more complex geometries that involve multiple contacts by linking with FE models.

Care must be taken when using NDT techniques carrying out such tests, as there are implications for design regarding the practicality, repeatability and reliability. This includes ensuring the testing technique is capable of identifying cracks which are relevant to the grain size of the group of materials being investigated. One technique might be more suitable for a material with a coarse grain size, but not for a finer grain size and therefore, a technique should be chosen that encompasses all the materials being investigated, to allow relevant comparisons to be made. For repeatability, some considerations for choosing the appropriate technique includes limited access to equipment, such as a high energy synchrotron beamline for XR, and if the equipment is hired, there is an increase in cost the more tests that need to be run. Furthermore, the reliability of some techniques still needs to be confirmed by repeat testing. For example, Hutson et al. [87] ran three repeat tests using shear wave ultrasound under the same loading conditions until failure, where one test was not able to detect crack initiation. This reduces the reliability of the method, as it was not able to detect crack initiation for each test. If crack propagation is the user's main priority, then methods, such as AE and PD, require crack growth calibration curves and these can vary with varying testing parameters and loading conditions. These curves are obtained using destructive methods or using in-situ microscopy methods, which reduces the efficiency if many different tests need to be run. If time is of concern, it should be noted that some techniques require interruptions to record images and alternative methods may be chosen to improve efficiency. In addition, for some NDT techniques, the test rig and specimen dimensions may need to be altered, which may not be practical for fretting fatigue tests under representative geometries and loading conditions. Other practicalities include ensuring that noise due to the contact does not interfere with the measurements, where reliability of filtering and processing methods are required.

In conclusion, these methods have their own limitations with regards to extensive testing for fretting fatigue life of components, which usually have a trade-off with increasing the fundamentals of fretting fatigue to improve modelling and life in the long run. It will depend on the user's priority, but in order to improve the usefulness of the data for design purposes, a standardisation for these tests should be a goal for the future to allow comparisons to be made between different materials, geometry and loading.

4. Recent developments in NDT techniques applicable for fretting fatigue

NDT techniques have been used in-situ with plain fatigue tests and have been used to observe pre-made fatigue cracks. This can show the capability of NDT techniques being used in-situ with fretting fatigue tests. The following shows the potential of X-ray radiography, ultrasound, thermography and acoustic emission techniques, as well as, alternative techniques such as laser ultrasound, moving mode of eddy-current thermography, eddy-current techniques and digital image correlation.

4.1. X-ray radiography

The potential of X-ray radiography can extend further with a 3D investigation of a fretting fatigue crack by using X-ray tomography. X-ray tomography involves collecting 2D X-ray radiographs at different angles of the specimen and a 3D image can be produced from these (see Fig. 29). This allows a further understanding of the formation of fretting fatigue cracks in 3D. This has been tested ex-situ with fretting fatigue and plain fatigue tests on pre-made fretting fatigue/plain fatigue cracks [120,122,123] and a 3D rendered image can be obtained from this. In-situ plain fatigue experiments have also been perfomed using X-ray tomography [146–151], where a 3D crack evolution was formed and investigated. Suggested future work will involve using 3D tomographic images in-situ with a fretting fatigue test to obtain more information on the multiple crack initiation sites and information on the 3D evolution of a fretting fatigue crack [85].

4.2. Ultrasound

The capability of traditional ultrasound techniques to be used within fretting fatigue testing can be shown by reviewing the works on using ultrasound in-situ for plain fatigue tests [140,145,152,153]. From these ultrasound tests, it was shown that the number of cycles to crack initiation can be identified and crack propagation can be monitored during plain fatigue tests. Recent works show that crack size can be evaluated after [153], as well as during [145], plain fatigue tests. Camacho et al. [145] were also able to evaluate the crack path and crack shape by developing a technique to produce images from the ultrasound wave response. This was achieved using an array of ultrasound transducer elements, known as ultrasound transducer arrays. Total focusing method (TFM) was used to obtain an image of the crack and phase coherence imaging (PCI) [154] was used to determine the crack length and crack tip location. TFM allows a single transducer element to be the transmitter, while all the transducer elements receive the receiving ultrasound wave response. This produces a single low resolution image. After this, a different transducer element is treated as the transmitter, which is then repeated until all the transducer elements are used as transmitters. This creates a collection of low resolution images, which are used create a high resolution image. The collection of signals from this are known as Full Matrix Capture (FMC). This method allows an image of the crack to be created, giving information about its crack path and orientation. Details on the TFM method can be found by Camacho et al. [145]; however, this method does not allow an accurate determination of the crack length, so PCI was used. Images were created using PCI focussing on the tips of the crack from the FMC. This allowed the distance between the crack tip and crack root to be accurately determined. Details on the PCI method can be found by Camacho et al. [145,154]. These imaging methods were used during a plain fatigue test and the images produced (see Fig. 30) proved to show a good agreement with optical measurements. These findings from plain fatigue tests show the potential of the ultrasound method.

4.2.1. Contactless ultrasound

Another ultrasound technique, known as laser ultrasound, can be used instead of the traditional ultrasound technique previously described. This is a promising technique overcoming the flaws of traditional ultrasound. This is a contactless technique that has greater sensitivity, being able to detect cracks at earlier stages than traditional ultrasound, as well as being able to pick up the location of cracks within a specimen [142,144]. Fig. 31 shows a schematic of the laser ultrasound technique. The following lists the steps of the laser ultrasound technique [142,144]:

1. A virtual grid is given to the specimen using a digital camera and computer software program.
2. The controller unit sends a signal to the excitation laser source to input an ultrasound wave to the specimen at the first virtual grid point.
3. The same ultrasound wave is picked up by the sensing unit from a Laser Doppler Vibrometer (LDV) for the first virtual grid point.
4. The data from the sensing unit is stored in the control unit.
5. The control unit repeats steps 2–4 until all the virtual grid points are evaluated.
6. Cracks are then detected from the data collected by the controller unit by counting the frequency- domain peaks out of the specified threshold.

This technique has been proved to be able to make an image of a notch in a plate by filtering the background noise of the cumulative ultrasound wave energy image by using an established threshold [144]. The cumulative ultrasound wave energy image is shown by Fig. 32a and the filtered image of the notch is shown by Fig. 32b. This allowed the location and the size of the notch to be determined. In addition, laser ultrasound has been tested on pre-made fatigue cracks on flat aluminium plates and aircraft fitting-lugs [142]. This shows that cracks can be inspected on samples with alternative geometries; however, incorporating this technique with a fatigue or fretting fatigue test has not yet been carried out and would entail further research to assess the feasibility of this technique. In addition, when using this technique, safety procedures and the affect of the laser on the surface of the specimen has yet to be taken into account [142].

4.3. Thermography

Thermography has been commonly used in-situ with plain fatigue tests [127,131,141,155–159]. Cycles to crack initiation has been found [156,157], as well as being able to locate crack initiation sites from thermal measurements and images [127,155,158].

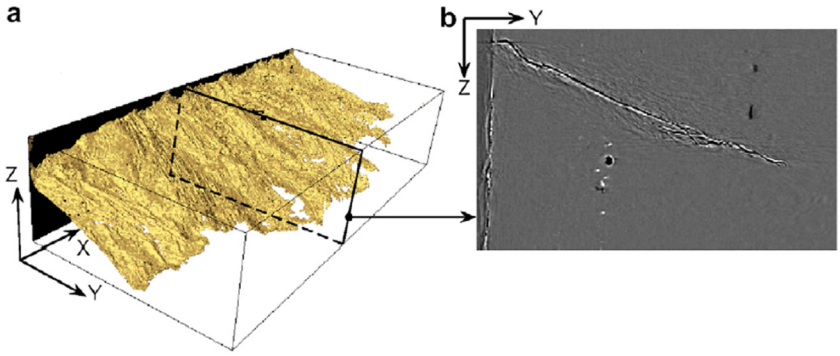

Fig. 29. (a) 3D rendered image of a fretting fatigue crack (b) 2D slice of the crack showing the crack path at this location [122].

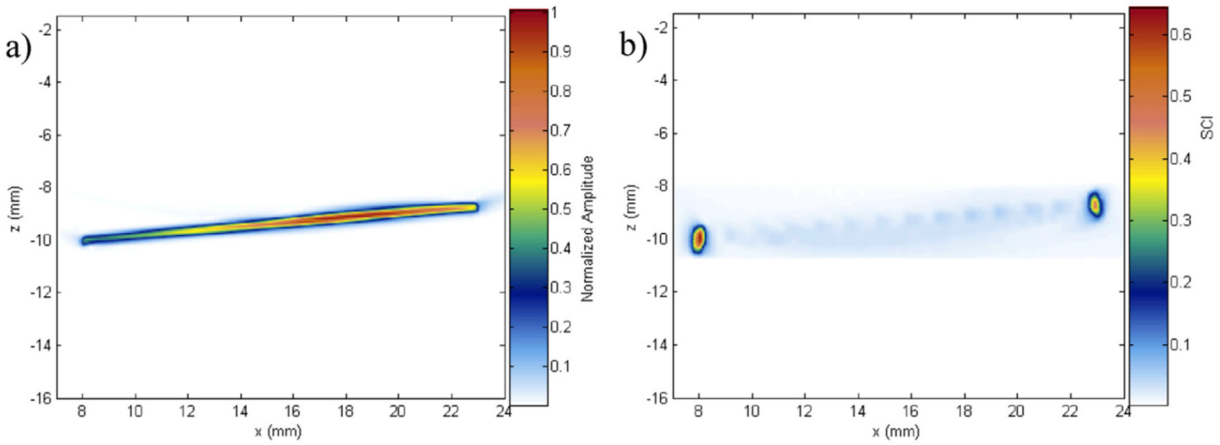

Fig. 30. Ultrasound images of a plain fatigue crack using a) TFM and b) PCI [145].

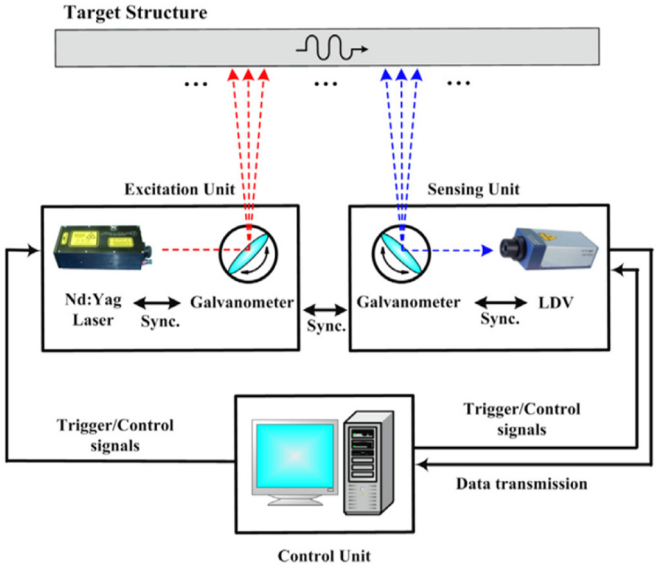

Fig. 31. Schematic diagram of a laser ultrasound set up [144].

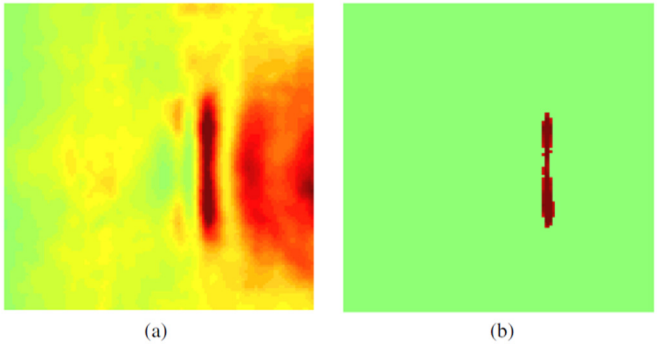

Fig. 32. (a) Cumulative ultrasound wave energy image and (b) the filtered image of a notch in a plate [144].

These thermal images give a great advantage over other techniques, as they provide a visual of the location of crack initiation (as shown in Fig. 33) and the crack path, which have been confirmed by SEM measurements [127]. The crack path is found by following the direction of the temperature at the crack tip [131]. Furthermore, it is also possible to determine the crack length [159]. In addition, Barile et al. [131] showed that thermography was a more efficient technique in localising and monitoring crack growth compared to AE. From these findings of thermography with in-situ plain fatigue tests, it is able to show the extent of information that can be collected using this technique.

Another thermography technique that can be proposed to inspect fretting fatigue crack is a technique recently tested by He et al. [160], which involves a moving flat specimen with a pre-made crack being heated by a stationary eddy current excitation source and stationary infrared camera to monitor the surface temperature over the specimen, as shown in Fig. 34. It was found that this method has many benefits, which included a high detection speed, clear thermal images of the crack and the determination of approximate crack locations; however, uneven surface emissivity can make it difficult to detect cracks and further research is required to investigate this, as well as incorporating this in-situ with a fretting fatigue test.

4.4. Acoustic emission

AE has been used in-situ with plain fatigue testing [97,119,140,161–164]. The number of cycles to crack initiation can be obtained [140,161–163], as well as the ability to distinguish between slow crack growth and fast crack growth using AE [161,162]. In addition, it was possible to determine how crack lengths changed with the number of cycles [97,119,161,164], by measuring the crack lengths during a fatigue test using a microscope for compact tension and T-section girder specimens. Keshtgar and Modarres [97] used AE with an optical microscope during a fatigue test of a compact tension specimen. The authors

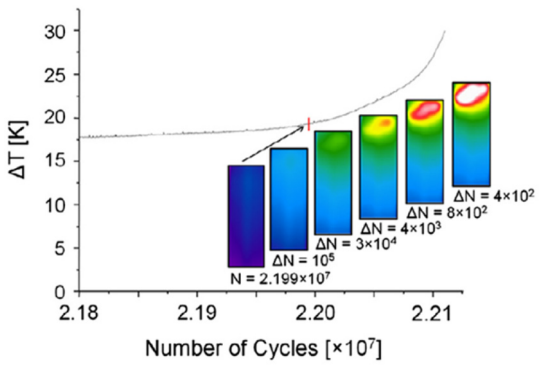

Fig. 33. Thermal measurements with thermal images of crack initiation at 2.199×10^7 cycles and the following crack growth [127].

found a linear relationship between the data from AE and the crack length measurements from the optical microscope. From this, it was possible to predict the crack initiation length. AE has, also, been used with SEM during a plain fatigue test to confirm the transitions in AE signals [119]. Futhermore, the crack rate could be determined using the Paris-Erdogan law and the acoustic emission count rate was predicted using a power law [164]. These equations were able to be used together to obtain the crack growth rate. These methods could be used in determining the initial crack size using AE with using SEM or OM during a fretting fatigue test and finding a relationship. AE would also compliment imagery methods in determining when crack initiation occurs. Difficulties would arise if cracks are internal and therefore, an alternative may be to use X-ray radiography to calibrate crack lengths to AE signals.

4.5. Eddy-current

The Eddy current technique involves the use of a coil carrying an alternating current near the specimen, whereby eddy-currents are induced into the specimen, as shown in Fig. 35. The magnetic flux is measured, changes in which indicate changes within the material, such as cracks [93]. Although it has not been used during a fretting fatigue experiment, it has been tested with plain fatigue experiments to detect crack initiation and monitor crack growth using eddy current arrays (multiple eddy current coils that are electronically driven) [165–168]. This technique proved to be highly sensitive in comparison with other techniques (see Fig. 23), as it can detect a minimum crack length of 25 μm [165,166]. In addition, the number of cycles to crack initiation can be determined [166,167]. Furthermore, Jiao et al. [167] was able to monitor crack length by placing multiple sensors along the specimen at a known distance. The eddy current distribution was measured at each sensor and changes indicated that either a crack has intiated or a crack has propagated. The distance from each sensor was known, so when the eddy current distribution was disturbed, it was known that the crack had elongated by the distance between the sensor, that has been disturbed, and the previous sensor, that has been previously disturbed. Another method used by Xie et al. [168] to monitor crack length involved an algorithm linking impedance and crack length.

Although a promising technique, this method would be difficult to use in-situ for a fretting fatigue test. Eddy current requires direct access to the crack (needing knowledge of the crack location) and it is not contactless, which proves difficult with already contacting surfaces. This would be especially difficult for large and complex contacting geometries. To overcome these issues, it could be possible to have an exterior moving eddy current coil that scans the specimen, similar to an experiment that used eddy current as the excitation source for a thermography experiment with a moving specimen to detect a crack [160]. This would need further work to check the feasibility of this method, as well as more research observing the crack propagation using the eddy current method. Other possible methods could include coupling with other NDT techniques to initially find the location of the crack to be monitored.

4.6. Digital image correlation

Digital image correlation (DIC) is a contactless optical method that uses a camera and lens system to take images of the specimen surface during a test and a displacement field is processed by calculating the displacements between images using a software, which are commercially available or custom-made. This method requires the specimen's surface to have a non-uniform contrasting speckled pattern, where under loading, the change in the speckle pattern can be measured and related to the displacement field. The speckle pattern can be produced artificially, such as spraying paint onto the surface, or it can be the natural texture of the surface due to the material itself. There are two types of DIC: two-dimensional (2D) and threedimensional (3D). 2D DIC is limited to specimens with a flat surface which measures in-plane deformations and only requires one camera, where the camera's axis is normal to the surface. Further details on 2D DIC has been reviewed by Pan et al. [169] and Zhao et al. [170]. 3D DIC can be used for specimens with a curved surface and measure out-of-plane deformations, which require two cameras. To take images using DIC, it has to be well illuminated by either a white light source or naturally illuminated. Furthermore, DIC has a wide range of sensitivity and resolution based on the camera and lens magnification, as well as the ability to be coupled up with microscopy methods [169,170]. DIC has been commonly used in-situ with fretting fatigue experiments to measure tangential displacements [171–174] using 2D DIC, slip displacements using 2D DIC [175,176] and 3D DIC [177], and the change in coefficient of friction [29] using 3D DIC; however, it has not been used with regards to crack initiation and crack propagation. For plain fatigue experiments, it has been used to detect cracks and examine crack growth [178–185], which shows the expanded capability of this method. The displacement field with the number of cycles is determined based on a reference image, which is typically when the specimen is undeformed at 0 cycles, and an image taken at a particular number of cycles. A crack is detected based on any discontinuities in the displacement field. The displacement field images allows the crack location, crack length and crack path to be determined with time. It has been possible to determine

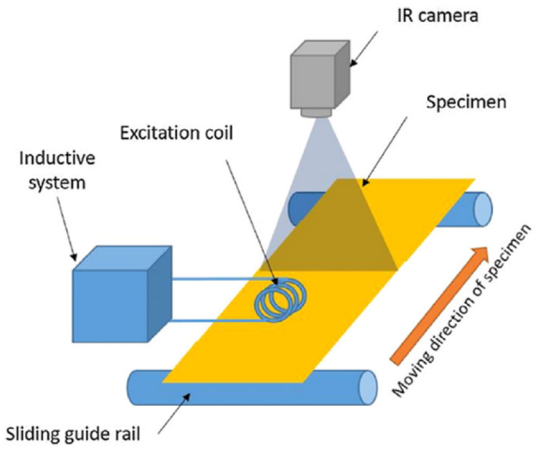

Fig. 34. Schematic diagram of the eddy current thermography method using a moving specimen [160].

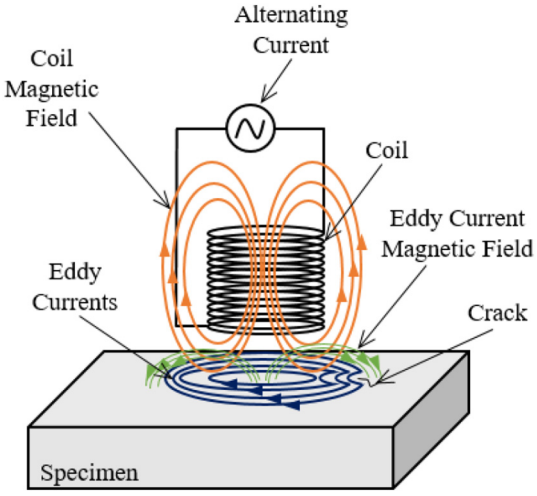

Fig. 35. Eddy current method schematic.

the number of cycles to crack initiation [178,180,181,185], crack location [178–185], crack growth curves [178–181,184,185], crack path [179–185] and obtain the stress intensity factor evolution at the crack tip [179,180,182–185]. DIC has been used to detect and locate fatigue microcracks as small as 0.6 μm [178]. This value is sub-pixel to the digital image, which is found based on sub-pixel algorithms, much more sensitive than using the raw images. Implementation of these methods for fretting fatigue is possible, as this technique has already been used to measure displacements, it can be expanded further for crack detection. However, care should be taken to limit error sources and ensure the field of view is visible. Some error sources include camera stability, errors due to the DIC algorithm itself, quality of the speckle pattern, various noises (e.g. illumination and noises associated with digital images), image distortions and the effect of out-of-plane motion for 2D DIC. Details of these error sources are found by Pan et al. [169] and Zhao et al. [170]. Furthermore, the imaging frequency should be optimised and the camera and lens magnification should be optimised for the size of the field of view and resolution required.

4.7. Implementation summary

NDT techniques that have been used in-situ with plain fatigue tests that can be applied to fretting fatigue tests have been described. The difficulties of implementation of these techniques and some possible solutions for these are summarised in Table 4.

5. Conclusions

NDT techniques have been reviewed for in-situ fretting fatigue tests to detect, locate and monitor fretting fatigue cracks. The NDT techniques reviewed were OM, SEM, XR, ultrasound, thermography, AE and DCPD techniques. Recent developments in NDT techniques for other applications applicable to fretting fatigue have also been discussed. The conclusions that can be drawn from the review are shown by the following:

- OM was found to be capable of satisfying all the main capabilities required for fretting fatigue testing due to providing images of crack evolution. Main drawbacks included that cycles to crack initiation was dependent on imaging frequency, crack initiation location detection relies on the user, limited to surface cracks and specimens are restricted for the field of view to be in the order of millimetres.
- SEM was also found to be capable of satisfying all the main requirements and had similar drawbacks to OM; however, SEM was able to capture microstructural features, such as slip lines and dislocation densities, which are important to obtain a deeper understanding of how and why fretting fatigue cracks form. Also, the main limitation was highlighted as adapting the fretting fatigue test to fit within the SEM vacuum chamber.
- XR was also able to satisfy all the main requirements. Similarly, the main drawbacks were that its sensitivity in detecting crack initiation is limited by its frequency of pausing the fretting fatigue test to take a radiograph and the synchrotron access has limited beam time, so tests have to be limited to a reduced number of cycles. It was also capable of detecting internal cracks, which are not possible with other imagery methods.
- The ultrasound technique is able to provide data on the number of cycles to crack initiation. The main limitations of this technique were that the sensitivity was the lowest in comparison with other techniques and the results of repeat tests varied. Further repeat tests are required to determine the suitability of this technique. Developments in other fields, where ultrasound imaging and laser ultrasound is possible, show there is scope to use the ultrasound technique in the future with fretting fatigue tests to detect crack initiation location and monitor crack evolution.
- Thermography is able to detect crack initiation location and determine the number of cycles to crack initiation in a timely manner from the use of infrared cameras. Thermography in-situ with fretting fatigue has not yet been used to evaluate crack propagation, so it has not yet been able to identify crack propagation modes, crack growth path and shape during a fretting fatigue test. A suggested improvement includes using higher resolution infrared image sensors to improve crack initiation sensitivity and possibly obtain the crack path. In addition, coupling with destructive techniques may be beneficial to obtain the crack propagation modes.
- The AE technique is a sensitive technique that is able to determine the number of cycles to crack initiation, identify crack propagation modes and detect crack location. AE has the potential to detect internal cracks, but is not capable of monitoring crack growth length, path and shape during fretting fatigue tests as of yet. Methods from plain fatigue tests to monitor crack growth length by calibrating AE signals with crack length measurements made by in-situ OM or SEM, or destructive methods could be used in the future.
- DCPD has commonly been able to determine the number of cycles to crack initiation for fretting fatigue tests. This technique allows the crack length to be monitored during the test using a calibration of potential drop results with destructive SEM tests. In addition, crack propagation modes can be identified from this. This technique is unable to detect the crack location, and prior knowledge of the crack location is required. This could be coupled up with OM or SEM to improve DCPD results.
- Choosing the most suitable NDT technique for in-situ fretting fatigue testing shall depend on what the user wants to achieve and considering each technique's limitations. For example, one user may want the technique with the lowest cost, where another may want the technique with the highest sensitivity.
- It was found from data for the number of cycles to crack initiation collected from the different NDT methods were limited. The data was collected from a variety of fretting fatigue experiments, which meant that a complete comparison of the NDT techniques could not be made. Therefore, to achieve a complete comparison, the same fretting fatigue test needs to be used with different NDT techniques to reach a conclusion with repeated tests to verify results. There are many variables that affect the cycles to crack initiation which include fretting loads, loading frequency, geometry, bulk stresses, material, surface modifications, coatings and microstructure. With this database, this could complete the comparison of these techniques, as well as gaining further knowledge on the efficiency of these NDT techniques and possibly how fretting fatigue cracks behave. There is the possibility of large amounts of future research that could investigate how these variables influence fretting fatigue, such as investigating how microstructures develop during fretting fatigue that may influence the presence of fretting fatigue cracks and the capability of NDT techniques being used for fretting fatigue tests with complex and component representative geometries (e.g. spline couplings, dovetails, railway axles, bolted joints, overhead conductors and wires).
- For design purposes, a standardisation for fretting fatigue tests should be a goal for the future to allow comparisons to be made between different materials, geometry and loading.
- Recent developments in NDT techniques applicable for fretting fatigue have been highlighted to show what other techniques are available that have been used for in-situ plain fatigue tests or pre-made cracks that could be applied to in-situ fretting fatigue tests. These included 3D X-ray tomography, ultrasound imaging techniques, laser ultrasound, passive thermography for crack propagation investigation, moving mode of eddy current thermography, AE crack growth calibration, eddy-current and DIC. Challenges of implementation and possible solutions were described. These techniques could be used as the scope for future research to expand the capability of NDT techniques in-situ with fretting fatigue tests.

Table 4
The challenges for the implementation of NDT techniques that could be applied to fretting fatigue.

NDT Technique	Refs.	Description	Challenges	Possible Design Solutions
X-Ray Tomography	[121,146–151]	Computed 3D image of a crack is developed using multiple 2D X-ray radiographs at different angles of the specimen. 3D crack evolution images can be computed	• Dimensions of the test rig and specimens are limited by the voxel resolution the user requires. For a higher resolution, smaller specimen sizes are needed to bring the specimen closer to the x-ray source [1211 • The penetration depth vary between different materials and the x-ray voltage [186]. The specimen should be orientated to reduce the variation in penetration depth during rotation scanning. For fretting fatigue, there would be additional material due to the extra applied loading and for the contacting pads. • Choose the appropriate tomography set up based on cost and scanning time, as scanning times are much longer for laboratory x-ray sources compared with a synchrotron beamline [121]. • The tests needs to be paused to take multiple radiographs (approximately 1200–1500 [146,149–151]) at different rotation angles limiting the duration of the fretting fatigue test due to the limited beam-time availability.	• Create a frame with a motor that can rotate the rig and direct any wires about the rotational axis. • Due to the penetration restrictions perpendicular to the pads, the angle of scanning rotation can be limited to obtain a tomographic image. Chapman et al. [146] were able to achieve this with a 140o scanning rotation for a high temperature fatigue test with a furnace, which restricted the field of view.
Ultrasound Imaging with TFM and PCI methods	[145]	Uses ultrasound transducer arrays which have multiple emitters and receivers along the specimen and using TFM and PCI methods, it is possible to process an image and accurate crack lengths using the ultrasound signals. 2D crack evolution ultrasound images could be achieved.	• Extra noise due to contact and additional loading need to be taken into account. • Ultrasound transducer array are wider than individual transducers due to the multiple emitters and receivers. Therefore positioning, attachment and ensuring no relative movement with the specimen needs to be carefully thought-out.	• If extra noise is an issue, it could be possible to pause tests to obtain the ultrasound image to limit the effects of noise due to contact and additional loads. If pausing undesirable, filtering these noises needs to be performed with care.
Contactless Laser Ultrasound	[142,144]	Uses two types of lasers: one as an emitter and the other as a receiver. The emitter laser scans the specimen and the receiver laser receives the ultrasound waves and outputs an image through automated post processing. 2D crack evolution ultrasound images could be achieved.	• Various background noises and additional noise due to loading and contact pads. • Ensure lasers are stable. • Emitter laser angle has little effect to the signal to noise ratio (SNR), whereas an increase in the receiver laser angle causes the SNR to deteriorate. These angles would need to be optimised to improve SNR.	• Tests may need to be paused to perform laser ultrasound scans, which can be used to limit noise due to contact and loading
Passive Thermography for Crack Propagation Investigation	[127,131,141,155,157,158]	Recording thermal images by using infrared cameras and obtaining thermal images of 2D crack evolution.	• Sources of noise due to room temperature, thermal losses, light intensity and contact. • Processing excess data for propagation may be difficult • Ensure stable ambient/room temperature • Ensure specimen's emissivity is not too low	• Methods have already been developed for fretting fatigue [94,130] for monitoring the temperature at region of interest during the test to determine the number of cycles to crack initiation including the filtering of various sources of noise. These methods can be applied for investigating crack propagation.
Eddy-Current Thermography	[160]	A specimen is heated by a stationary eddy-current source, which moves past an infrared camera that monitors the temperature over the specimen's surface. Using a heat source, this can reduce the ambient temperature effects. This could potentially produce thermal images of 2D crack evolution.	• Ensure eddy-current source is near the crack, which would be difficult for tests that involve multiple contacts and edges. • Moving the specimen for the infrared camera would be difficult. • Require eddy-current source does not block field of view. • Ensure that mounting the eddy-current source to the specimen does not influence the fretting fatigue result. • Ensure temperature produced by the eddy-current is stable.	• Stationary mode eddy- current thermography would be viable [159], as there is a small area of interest. Moving mode is more applicable to large scale components. • Although not trivial, create a bespoke eddy-current sensors suited for the geometry to ensure this does not block the field of view, while near the region of possible crack initiation. For example, Jiao et al. [167], created an eddy-current sensor for fatigue of a bolted joint that fits beneath a custom washer.
AE Crack Growth Calibration	[97,119,164]	Obtain a calibration curve for crack growth either by using a microscopy technique or using the Paris-Erdogan law.	• If using optical microscopy, ensure the specimen is illuminated. • If using SEM, the challenges include: fitting the experimental set up within a vacuum chamber, which would involve the use of miniature specimens; the	• Optical microscope would be ideal for crack length measurements with regards to cost and ease of implementation.

(continued on next page)

Table 4 (*continued*)

NDT Technique	Refs.	Description	Challenges	Possible Design Solutions
			associated microstructure and specimen size interaction issues; the addition of using AE; and the significant increase in cost would have to be considered. • If using a correlation based on the Paris-Erdogan law, a feasibility study would need to be made, as it may not be applicable under various parameters for fretting fatigue.	
Eddy-Current	[165–168]	Eddy-current sensors are positioned along the specimen and any disturbance in the magnetic flux indicates a crack. The approximate crack length can be found from the distance between sensors. This method allows the detection of crack initiation, crack growth measurements and 2D permeabil- ity/impedance images of crack with a scanning eddy current arrays.	• Need approximate location of the crack for sensors, which would be difficult for tests that involve multiple contacts and edges. • Optimisation of the location and positioning between sensors or the sensors used. • Ensure that mounting the sensors to the specimen does not influence the fretting fatigue result.	• Make use of eddy-current arrays.
Digital Image Correlation	[178,181,182,184,185,187]	Speckled specimens are imaged using a camera and lens system and measurements of the displacement field can be found through changes in the speckled pattern images. Detection of microcracks can be determined and 2D crack evolution images can be found	• Stable white light source to illuminate specimen. • Need to ensure the specimen prepping procedure does not affect the contacting surfaces. • If specimens are prepped with paint, it would prevent the earlier detection of cracks before it breaks through the paint to be visible [178]. • Surface of sample must be a flat plane and perpendicular to the camera's axis. • Require field of view is visible. • Optimise imaging frequency, illumination and the resulting contrast needs to be confirmed.	• Imaging methods have been applied with fretting fatigue tests, so obstruction of the field of view should not be an issue. • It has been commonly used to perform DIC without the use of applying an artificial speckle pattern on the specimen's surface, as it relies on the natural texture of the material giving a random grey intensity distribution [169,178,184,185,187]. Rupil et al. [178] relied on the specimen's material being polycrystalline and surface roughening of persistent slip bands to perform, where using the author's DIC algorithm was able to detect micro cracks.

Declaration of Competing Interest

None.

Acknowledgement

The authors would like to acknowledge the Engineering and Physical Science Research Council (Grant EP/P510592/1) and Rolls-Royce plc for providing financial support for this work.

References

[1] F. Eden, E.M. Rose, W.N. Cunningham, The endurance of metals: experiments on rotating beams at university college, London, Proc. Inst. Mech. Engrs. 875 (1) (1911) 839–974.
[2] D.S. Wei, S.H. Yuan, Y.R. Wang, Failure analysis of dovetail assemblies under fretting load, Eng. Fail. Anal. 26 (2012) 381–396.
[3] R. Rajasekaran, D. Nowell, Fretting fatigue in dovetail blade roots: Experiment and analysis, Tribo. Int. 39 (2006) 1277–1285 oct.
[4] C. Ruiz, P.H. Boddington, K.C. Chen, An investigation of fatigue and fretting in a dovetail joint, Exp. Mech. 24 (3) (1984) 208–217.
[5] J.J. Madge, S.B. Leen, P.H. Shipway, The critical role of fretting wear in the analysis of fretting fatigue, Wear 263 (2007) 542–551.
[6] K. Makino, S. Biwa, H. Sakamoto, J. Yohso, Ultrasonic evaluation of fatigue cracks at the wheel seat of a miniature wheelset, Nondestruct. Test. Eval. 27 (1) (2012) 29–46.
[7] M. Luke, M. Burdack, S. Moroz, I. Varfolomeev, Experimental and numerical study on crack initiation under fretting fatigue loading, Int. J. Fatigue 86 (2016) 24–33.
[8] V. Linhart, I. Černý, An effect of strength of railway axle steels on fatigue resistance under press fit, Eng. Fracture Mech. 78 (2011) 731–741 mar.
[9] M.B. Marshall, R. Lewis, R.S. Dwyer-Joyce, Characterisation of contact pressure distribution in bolted joints, Strain 42 (2006) 31–43 feb.
[10] S. Wagle, H. Kato, Ultrasonic wave intensity reflected from fretting fatigue cracks at bolt joints of aluminum alloy plates, NDT E Int. 42 (2009) 690–695.
[11] C.R. Azevedo, T. Cescon, Failure analysis of aluminum cable steel reinforced (ACSR) conductor of the transmission line crossing the Paraná River, Eng. Failure Anal. 9 (2002) 645–664 dec.
[12] A.A. Fadel, D. Rosa, L.B. Murça, J.L. Fereira, J.A. Araújo, Effect of high mean tensile stress on the fretting fatigue life of an Ibis steel reinforced aluminium conductor, Int. J. Fatigue 42 (2012) 24–34 sep.
[13] M.S. Pestana, R.B. Kalombo, R.C.S. Freire Júnior, J.L.A. Ferreira, C.R.M. da Silva, J.A. Araújo, Use of artificial neural network to assess the effect of mean stress on fatigue of overhead conductors, Fatigue Fract. Eng. Mater. Struct. 41 (12) (2018) 2577–2586.
[14] S. Lalonde, R. Guilbault, S. Langlois, Numerical analysis of ACSR conductor-clamp systems undergoing wind-induced cyclic loads, IEEE Transac. Power Deliv. 33 (4) (2018) 1518–1526.
[15] B. Berthel, A.R. Moustafa, E. Charkaluk, S. Fouvry, Crack nucleation threshold under fretting loading by a thermal method, Tribol. Int. 76 (2014) 35–44.
[16] O. Vingsbo, D. Soderberg, On Fretting Maps, Wear1 126 (2) (1988) 131–147.
[17] D.A. Hills, D. Nowel, Mechanics of Fretting Fatigue, Springer Science & Business Media, Berlin, 1994.
[18] D. Nowell, D. Dini, D.A. Hills, Recent developments in the understanding of fretting fatigue, Eng. Fract. Mech. 73 (2006) 207–222.
[19] F. Abbasi, G. Majzoobi, M. Barjesteh, Developing a new experimental set up to study fretting fatigue behavior under cyclic contact loading, Proceed. Instit. Mech. Eng. Part J (2017) 1–14.
[20] D. Wang, D. Zhang, S. Ge, Effect of displacement amplitude on fretting fatigue behavior of hoisting rope wires in low cycle fatigue, Tribol. Int. 52 (2012) 178–189.
[21] S.A. Namjoshi, S. Mall, V.K. Jain, O. Jin, Fretting fatigue crack initiation mechanism in Ti-6Al-4V, Fatigue & Fracture of Engineering Materials & Structures, 25, 2002, pp. 955–964 , oct.
[22] S. Fouvry, H. Gallien, B. Berthel, From uni- to multi-axial fretting-fatigue crack nucleation: development of a stress-gradient-dependent critical distance approach, Int. J. Fatigue 62 (2014) 194–209.
[23] N.A. Bhatti, M.A. Wahab, Fretting fatigue crack nucleation: a review, Tribiol. Int. 121 (2018) 121–138.
[24] J. Vázquez, C. Navarro, J. Domínguez, Analysis of fretting fatigue initial crack path in Al7075-T651 using cylindrical contact, Tribiol. Int. 108 (2017) 87–94.
[25] N.A. Bhatti, M. Abdel Wahab, A continuum damage mechanics approach for fretting fatigue under out of phase loading, Tribol. Int. 121 (2018) 204–213.

[26] N.A. Bhatti, M. Abdel Wahab, Fretting fatigue damage nucleation under out of phase loading using a continuum damage model for non-proportional loading, Tribol. Int. 121 (2018) 204–213.
[27] N.A. Bhatti, M. Abdel Wahab, A numerical investigation on critical plane orientation and initiation lifetimes in fretting fatigue under out of phase loading conditions, Tribol. Int. 115 (2017) 307–318.
[28] O.J. McCarthy, J.P. McGarry, S.B. Leen, Micro-mechanical modelling of fretting fatigue crack initiation and wear in Ti-6Al-4V, Int. J. Fatigue 62 (2014) 180–193.
[29] R. Hojjati-Talemi, M. Abdel Wahab, J. De Pauw, P. De Baets, Prediction of fretting fatigue crack initiation and propagation lifetime for cylindrical contact configuration, Tribol. Int. 76 (2014) 73–91.
[30] R. Hojjati-Talemi, M.A. Wahab, Fretting fatigue crack initiation lifetime predictor tool: using damage mechanics approach, Tribol. Int. 60 (2013) 176–186.
[31] K. Pereira, M. Abdel Wahab, Fretting fatigue crack propagation lifetime prediction in cylindrical contact using an extended MTS criterion for non-proportional loading, Tribol. Int. 115 (2017) 525–534.
[32] R.A. Cardoso, T. Doca, D. Néron, S. Pommier, J.A. Araújo, Wear numerical assessment for partial slip fretting fatigue conditions, Tribol. Int. 136 (2019) 508–523 aug.
[33] J.A. Araújo, F.C. Castro, I.M. Matos, R.A. Cardoso, Life prediction in multiaxial high cycle fretting fatigue, Int. J. Fatigue 134 (2020) 105504 may.
[34] D. Houghton, P.M. Wavish, E.J. Williams, S.B. Leen, Multiaxial fretting fatigue testing and prediction for splined couplings, Int. J. Fatigue 31 (2009) 1805–1815.
[35] M. Ciavarella, A 'crack-like' notch analogue for a safe-life fretting fatigue design methodology, Fatigue Fract. Eng. Mater. Struct. 26 (2003) 1159–1170.
[36] O.J. McCarthy, J.P. McGarry, S.B. Leen, The effect of grain orientation on fretting fatigue plasticity and life prediction, Tribol. Int. 76 (2014) 100–115.
[37] F. Abbasi, G.H. Majzoobi, An investigation into the effect of elevated temperatures on fretting fatigue response under cyclic normal contact loading, Theor. Appl. Fract. Mech. 93 (2018) 144–154.
[38] C.D. Lykins, S. Mall, V. Jain, An evaluation of parameters for predicting fretting fatigue crack initiation, Int. J. Fatigue 22 (2000) 703–716.
[39] J.A. Araújo, D. Nowell, The effect of rapidly varying contact stress fields on fretting fatigue, Int. J. Fatigue 24 (2002) 763–775.
[40] W.S. Sum, E.J. Williams, S.B. Leen, Finite element, critical-plane, fatigue life prediction of simple and complex contact configurations, Int. J. Fatigue 27 (2005) 403–416.
[41] J. Ding, S.B. Leen, E.J. Williams, P.H. Shipway, Finite element simulation of fretting wear- fatigue interaction in spline couplings, Tribol. Mater. Surf. Interfaces 2 (1) (2008) 10–24.
[42] J. Ding, W.S. Sum, R. Sabesan, S.B. Leen, I.R. McColl, E.J. Williams, Fretting fatigue predictions in a complex coupling, Int. J. Fatigue 29 (7) (2007) 1229–1244.
[43] J. Ding, D. Houghton, E.J. Williams, S.B. Leen, Simple parameters to predict effect of surface damage on fretting fatigue, Int. J. Fatigue 33 (2011) 332–342.
[44] P.M. Wavish, D. Houghton, J. Ding, S.B. Leen, E.J. Williams, I.R. McColl, A multiaxial fretting fatigue test for spline coupling contact, Fatigue Fract. Eng. Mater. Struct. 32 (2009) 325–345.
[45] C. Gandiolle, S. Fouvry, FEM modeling of crack nucleation and crack propagation fretting fatigue maps: plasticity effect, Wear 330-331 (2015) 136–144.
[46] R. Ferre, S. Fouvry, B. Berthel, R. Amargier, J.A. Ruiz-Sabariego, Prediction of the fretting fatigue crack nucleation endurance of a Ti-6V-4Al/ Ti-6V-4Al interface: influence of plasticity and tensile/shear fatigue properties, Procedia Eng. 66 (2013) 803–812.
[47] G.M. Almeida, G.C. Pessoa, R.A. Cardoso, F.C. Castro, J.A. Araújo, et al., Tribol. Int. 144 (2020) 106103 apr.
[48] S. Vantadori, G.M.J. Almeida, G. Fortese, G.C.V. Pessoa, J.A. Araújo, Early fretting crack orientation by using the critical plane approach, Int. J. Fatigue 114 (2018) 282–288.
[49] M. Marco, D. Infante-García, J. Díaz-Álvarez, E. Giner, Relevant factors affecting the direction of crack propagation in complete contact problems under fretting fatigue, Tribol. Int. 131 (2019) 343–352 mar.
[50] K. Pereira, N. Bhatti, M. Abdel Wahab, Prediction of fretting fatigue crack initiation location and direction using cohesive zone model, Tribol. Int. 127 (2018) 245–254.
[51] J.C. Martínez, L.V. Vanegas Useche, M.A. Wahab, Numerical prediction of fretting fatigue crack trajectory in a railway axle using XFEM, Int. J. Fatigue 100 (2017) 32–49.
[52] M.C. Baietto, E. Pierres, A. Gravouil, A multi-model X-FEM strategy dedicated to frictional crack growth under cyclic fretting fatigue loadings, Int. J. Solids Struct. 47 (2010) 1405–1423.
[53] M.C. Baietto, E. Pierres, A. Gravouil, B. Berthel, S. Fouvry, B. Trolle, Fretting fatigue crack growth simulation based on a combined experimental and XFEM strategy, Int. J. Fatigue 47 (2013) 31–43.
[54] C. Navarro, S. Muñoz, J. Domínguez, On the use of multiaxial fatigue criteria for fretting fatigue life assessment, Int. J. Fatigue 30 (1) (2008) 32–44.
[55] C. Navarro, J. Vázquez, J. Domínguez, Nucleation and early crack path in fretting fatigue, Int. J. Fatigue 100 (2017) 602–610.
[56] A. Ferjaoui, T. Yue, M. Abdel Wahab, R. Hojjati-Talemi, Prediction of fretting fatigue crack initiation in double lap bolted joint using continuum damage mechanics, Int. J. Fatigue 73 (2015) 66–76.
[57] S. Fouvry, P. Duó, P. Perruchaut, A quantitative approach of Ti-6Al-4V fretting damage: friction, wear and crack nucleation, Wear 257 (2004) 916–929.
[58] F. Aguirre, C. Vallellano, J. Domínguez, On the application of a micromechanical small fatigue crack growth model to predict fretting fatigue life in AA7075-T6 under spherical contact, Tribol. Int. 76 (2014) 6–13.
[59] A. de Pannemaecker, S. Fouvry, J.Y. Buffiere, M. Brochu, Modelling the fretting fatigue crack growth: from short crack correction strategies to microstructural approaches, Int. J. Fatigue 117 (2018) 75–89.
[60] P. Paris, F. Erdogan, Critical analysis of crack propagation laws, J. Basic Eng. 85 (1963) 528–533.
[61] M. El Haddad, T. Topper, K. Smith, Prediction of non-propagating cracks, Eng. Fract. Mech. 11 (3) (1979) 573–584.
[62] C. Gandiolle, S. Fouvry, E. Charkaluk, Lifetime prediction methodology for variable fretting fatigue loading: plasticity effect, Int. J. Fatigue 92 (2016) 531–547.
[63] P. Arnaud, S. Fouvry, S. Garcin, Wear rate impact on Ti-6Al-4V fretting crack risk: experimental and numerical comparison between cylinder/plane and punch/plane contact geometries, Tribol. Int. 108 (2017) 32–47.
[64] C. Gandiolle, S. Fouvry, Experimental analysis and modeling of the crack arrest condition under severe plastic fretting fatigue conditions, Procedia Eng. 66 (2013) 783–792.
[65] J. Meriaux, S. Fouvry, K.J. Kubiak, S. Deyber, Characterization of crack nucleation in TA6V under fretting-fatigue loading using the potential drop technique, Int. J. Fatigue 32 (2010) 1658–1668.
[66] J. Meriaux, M. Boinet, S. Fouvry, J.C. Lenain, Identification of fretting fatigue crack propagation mechanisms using acoustic emission, Tribol. Int. 43 (2010) 2166–2174.
[67] R. Prakash, Non-Destructive Testing Techniques, New Academic Science, Kent, 2011.
[68] M. Ratassepp, J. Rao, Z. Fan, Quantitative imaging of Young's modulus in plates using guided wave tomography, NDT E Int. 94 (2018) 22–30.
[69] T. Garcin, J.H. Schmitt, M. Militzer, In-situ laser ultrasonic grain size measurement in superalloy INCONEL 718, J. Alloys Compd. 670 (2016) 329–336.
[70] P.R. Arora, M.S. Jacob, M.S. Salit, E.M. Ahmed, M. Saleem, P. Edi, Experimental evaluation of fretting fatigue test apparatus, Int. J. Fatigue 29 (5) (2007) 941–952.
[71] J. Muthu, Fatigue life of 7075-T6 aluminium alloy under fretting condition, Theor. Appl. Fract. Mech. 74 (1) (2014) 200–208.
[72] J. Larsen, J. Jira, K. Ravichandran, Measurement of small cracks by Photomicroscopy: Experiments and analysis, in: J.M. Larson, J.E. Allison (Eds.), Small-Crack Test Methods, American Society for Testing and Materials International, Philadelphia, PA 1992, pp. 57–80.
[73] G.H. Majzoobi, K. Azadikhah, J. Nemati, The effects of deep rolling and shot peening on fretting fatigue resistance of Aluminum-7075-T6, Mater. Sci. Eng. A 516 (1–2) (2009) 235–247.
[74] G.H. Majzoobi, F. Abbasi, On the effect of shot-peening on fretting fatigue of Al7075-T6 under cyclic normal contact loading, Surf. Coat. Technol. 328 (2017) 292–303.
[75] H.K. Jeung, J.D. Kwon, C.Y. Lee, Crack initiation and propagation under fretting fatigue of inconel 600 alloy, J. Mech. Sci. Technol. 29 (12) (2015) 5241–5244.
[76] Y. Su, Q.N. Han, W. Qiu, Z. He, Y.B. Shang, H.J. Shi, L.S. Niu, High temperature in-situ SEM observation and crystal plasticity simulation on fretting fatigue of Ni-based single crystal superalloys, Int. J. Plast. 127 (2020) 102645.
[77] Q.N. Han, S.S. Rui, W. Qiu, Y. Su, X. Ma, Z. He, H. Cui, H. Zhang, H.J. Shi, Subsurface crack formation and propagation of fretting fatigue in Ni-based single-crystal superalloys, Fatigue Fract. Eng. Mater. Struct. 42 (2019) 2520–2532.
[78] Q.N. Han, W. Qiu, Z. He, Y. Su, X. Ma, H.J. Shi, The effect of crystal orientation on fretting fatigue crack formation in Ni-based single-crystal superalloys: in-situ SEM observation and crystal plasticity finite element simulation, Tribol. Int. 125 (2018) 209–219.
[79] Q.N. Han, W. Qiu, Y.B. Shang, H.J. Shi, In-situ SEM observation and crystal plasticity finite element simulation of fretting fatigue crack formation in Ni-base single-crystal superalloys, Tribol. Int. 101 (2016) 33–42.
[80] Q.N. Han, S.S. Rui, W. Qiu, X. Ma, Y. Su, H. Cui, H. Zhang, H. Shi, Crystal orientation effect on fretting fatigue induced geometrically necessary dislocation distribution in Ni-based single-crystal superalloys, Acta Mater. 179 (2019) 129–141.
[81] T. Nishida, K. Kondoh, J.-Q. Xu, Y. Mutoh, E. Kanyon, D.W. Hoeppner, S. Mutoh, Y. Hoeppner, D. Kinyon, Observations and analysis of relative slip in fretting fatigue, Fretting Fatigue: Advances in Basic Understanding and Applications, ASTM International, West Conshohocken, PA 2003, pp. 33–43.
[82] A. Ul-Hamid, A Beginners' Guide to Scanning Electron Microscopy, Springer Nature Switzerland, Cham, Switzerland, 2018.
[83] L. Zhang, S. Ma, D. Liu, B. Markert, Fretting wear modelling incorporating cyclic ratcheting deformations and the debris evolution for Ti-6Al-4V, Tribiol. Int. 136 (2019) 317–331.
[84] P.J. Shull, Nondestructive Evaluation, Marcel Dekker, Inc., New York, 2002.
[85] A. De Pannemaecker, J.Y. Buffiere, S. Fouvry, O. Graton, In situ fretting fatigue crack propagation analysis using synchrotron X-ray radiography, Int. J. Fatigue 97 (2017) 56–69.
[86] C. Meola, Recent Advances in Non-Destructive Inspection, Nova Science Publishers, Inc, New York, 2010.
[87] A.L. Hutson, N.E. Ashbaugh, T. Nicholas, S.E. Kinyon, D.W. Hoeppner, An investigation of fretting fatigue crack nucleation life of Ti-6AI-4V under flat-on-flat contact, in: Y. Mutoh, S.E. Kinyon, D.W. Hoeppner (Eds.), Fretting Fatigue: Advances in Basic Understanding and Applications, ASTM International, West Conshohocken, PA 2003, pp. 307–322.
[88] A.L. Hutson, D. Stubbs, A fretting fatigue crack detection feasibility study using shear wave non-destructive inspection, Exp. Mech. 45 (2) (2005) 160–166.
[89] X. Jian, S. Smalley, J. Knowles, R. Moser, K. Quirk, Fretting cracking ultrasonic detection in generator teeth, *17th World Conference on Nondestructive Testing,* (Shanghai), 2008 , NDT.
[90] C. Ibarra-Castanedo, J.R. Tarpani, X.P.V. Maldague, Nondestructive testing with thermography, Eur. J. Phys. 34 (6) (2013) S91–S109.

[91] Y.Y. Hung, Y.S. Chen, S.P. Ng, L. Liu, Y.H. Huang, B.L. Luk, R.W. Ip, C.M. Wu, P.S. Chung, Review and comparison of shearography and active thermography for nondestructive evaluation, Mater. Sci. Eng. R 64 (2009) 73–112.
[92] C.L. Neslen, S. Mall, S. Sathish, Nondestructive characterization of fretting fatigue damage, J. Nondestruct. Eval. 23 (4) (2004) 153–162.
[93] D.S. Forsyth, M. Genest, J. Shaver, T.B. Mills, Evaluation of nondestructive testing methods for the detection of fretting damage, Int. J. Fatigue 29 (2007) 810–821.
[94] S. Chhith, W. De Waele, P. De Baets, T.V. Hecke, On-line detection of fretting fatigue crack initiation by lock-in thermography, Tribiol. Int. 106 (2017) 150–155.
[95] S. Chhith, W. De Waele, P. De Baets, Rapid determination of fretting fatigue limit by infrared thermography, Exp. Mech. 58 (2018) 259–267.
[96] C.U. Grosse, M. Ohtsu, Acoustic Emission Testing, Springer-Verlag Verlin Geidelberg 2008.
[97] A. Keshtgar, M. Modarres, Detecting crack initiation based on acoustic emission, Chem. Eng. 33 (2013) 547–552.
[98] A. Cadario, B. Alfredsson, Fretting fatigue crack growth for a spherical indenter with constant and cyclic bulk load, Eng. Fract. Mech. 72 (2005) 1664–1690.
[99] A. Cadario, B. Alfredsson, Fretting fatigue experiments and analyses with a spherical contact in combination with constant bulk stress, Tribol. Int. 39 (2006) 1248–1254.
[100] D. Wang, D. Zhang, S. Ge, Fretting-fatigue behavior of steel wires in low cycle fatigue, Mater. Des. 32 (2011) 4986–4993.
[101] G. Sposito, Advances In Potential Drop Techniques for Non-Destructive Testing, PhD thesis Imperial College London, 2009.
[102] C. Gandiolle, S. Fouvry, Fretting fatigue crack propagation rate under variable loading conditions, Fracture Struct. Integrity 35 (2016) 232–241.
[103] Y. Kondo, C. Sakae, M. Kubota, K. Yanagihara, Non-propagating crack behaviour at giga-cycle fretting fatigue limit, Fatigue Fract. Eng. Mater. Struct. 28 (2005) 501–506.
[104] M. Kubota, K. Kuwada, Y. Tanaka, Y. Kondo, Mechanism of reduction of fretting fatigue limit caused by hydrogen gas in SUS304 austenitic stainless steel, Tribiol. Int. 44 (2011) 1495–1502.
[105] G.H. Majzoobi, A.R. Ahmadkhani, The effects of multiple re-shot peening on fretting fatigue behavior of Al7075-T6, Surf. Coat. Technol. 205 (1) (2010) 102–109.
[106] G.H. Majzoobi, J. Nemati, A.J. Novin Rooz, G.H. Farrahi, Modification of fretting fatigue behavior of AL7075-T6 alloy by the application of titanium coating using IBED technique and shot peening, Tribol. Int. 42 (1) (2009) 121–129.
[107] G.H. Majzoobi, M. Jaleh, Duplex surface treatments on AL7075-T6 alloy against fretting fatigue behavior by application of titanium coating plus nitriding, Mater. Sci. Eng. A 452–453 (2007) 673–681.
[108] F. Abbasi, G.H. Majzoobi, Effect of out-of-phase loading on fretting fatigue response of Al7075-T6 under cyclic normal loading using a new testing apparatus, Eng. Fract. Mech. 188 (2018) 93–111.
[109] X. Ma, H. Shi, J. Gu, G. Chen, O. Luesebrink, H. Hardersd, In-situ observations of the effects of orientation and carbide on low cycle fatigue crack propagation in a single crystal superalloy, Procedia Eng. 2 (1) (2010) 2287–2295.
[110] X. Ma, H.J. Shi, J. Gu, In-situ scanning electron microscopy studies of small fatigue crack growth in recrystallized layer of a directionally solidified superalloy, Mater. Lett. 64 (19) (2010) 2080–2083.
[111] J. Liang, Z. Wang, H. Xie, H. Shi, X. Li, In situ scanning electron microscopy analysis of effect of temperature on small fatigue crack growth behavior of nickel-based single-crystal superalloy, Int. J. Fatigue 128 (105195) (2019) 1–13.
[112] L. Yan, J.K. Fan, In-situ SEM study of fatigue crack initiation and propagation behavior in 2524 aluminum alloy, Mater. Des. 110 (2016) 592–601.
[113] Y.B. Shang, H.J. Shi, Z.X. Wang, G.D. Zhang, In-situ SEM study of short fatigue crack propagation behavior in a dissimilar metal welded joint of nuclear power plant, Mater. Des. 88 (2015) 598–609.
[114] Y. Zhang, L. You, X. Li, J. Zhou, X. Song, In-situ investigation of the fatigue crack initiation and propagation behavior of Zircaloy-4 with different hydrogen contents at RT and 300C, J. Nucl. Mater. 532 (2020) 152065.
[115] A. Ahmadi, F. Sadeghi, S. Shaffer, In-situ friction and fretting wear measurements of Inconel 617 at elevated temperatures, Wear 410–411 (2018) 110–118.
[116] Y. Otsuka, Y. Miyashita, Y. Mutoh, Effects of delamination on fretting wear behaviors of plasma-sprayed hydroxyapatite coating, Mech. Eng. J. 3 (2) (2016) 1–11.
[117] E.A. Torres, A.J. Ramírez, In situ scanning electron microscopy, Sci. Technol. Weld. Join. 16 (1) (2011) 68–78.
[118] W. Kang, M. Merrill, J.M. Wheeler, In situ thermomechanical testing methods for micro/nano-scale materials, Nanoscale 9 (8) (2017) 2666–2688.
[119] B. Wisner, M. Cabal, P.A. Vanniamparambil, J. Hochhalter, W.P. Leser, A. Kontsos, In situ microscopic investigation to validate acoustic emission monitoring, Exp. Mech. 55 (9) (2015) 1705–1715.
[120] H. Proudhon, J.-Y. Buffière, S. Fouvry, Characterisation of fretting fatigue damage using synchrotron X-ray micro-tomography, Tribol. Int. 39 (2006) 1106–1113.
[121] J.Y. Buffiere, E. Maire, J. Adrien, J.P. Masse, E. Boller, In situ experiments with X ray tomography: An attractive tool for experimental mechanics, Exp. Mech. 50 (2010) 289–305.
[122] H. Proudhon, J.-Y. Buffière, S. Fouvry, Three-dimensional study of a fretting crack using synchrotron X-ray micro-tomography, Eng. Fract. Mech. 74 (2007) 782–793.
[123] J.Y. Buffiere, E. Ferrie, H. Proudhon, W. Ludwig, Three-dimensional visualisation of fatigue cracks in metals using high resolution synchrotron X-ray microtomography, Mater. Sci. Technol. 22 (9) (2006) 1019–1024.
[124] L. Cartz, Nondestructive Testing, ASM International, Russell Township, 1995.
[125] S. Wagle, H. Kato, Real-time measurement of ultrasonic waves at bolted joints under fatigue testing, Exp. Mech. 51 (9) (2011) 1559–1564.
[126] A.L. Hutson, C. Neslen, T. Nicholas, Characterization of fretting fatigue crack initiation processes in CR Ti-6Al-4V, Tribol. Int. 36 (2003) 133–143.
[127] D. Krewerth, A. Weidner, H. Biermann, Application of in situ thermography for evaluating the high-cycle and very high-cycle fatigue behaviour of cast aluminium alloy AlSi7Mg (T6), Ultrasonics 53 (2013) 1441–1449.
[128] K.N. Pandey, S. Chand, Analysis of temperature distribution near the crack tip under constant amplitude loading, Fatigue Fract. Eng. Mater. Struct. 31 (2008) 316–326.
[129] A.Y. Fedorova, M.V. Bannikov, O.A. Plekhov, Infrared thermography study of the fatigue crack propagation, Frattura ed Integrità Strutturale 21 (2012) 46–53.
[130] S. Chhith, Experimental Methodologies to Study Fretting Fatigue Damage and Crack Initiation, PhD thesis Ghent University, 2017.
[131] C. Barile, C. Casavola, G. Pappalettera, C. Pappalettere, Analysis of crack propagation in stainless steel by comparing acoustic emissions and infrared thermography data, Eng. Fail. Anal. 69 (2015) 35–42.
[132] P. Hellstein, M. Szwedo, 3D thermography in non-destructive testing of composite structures, Meas. Sci. Technol. 27 (124006) (2016) 1–12.
[133] Z. Nazarchuk, V. Skalskyi, O. Serhiyenko, Propagation of elastic waves in solids, Acoustic Emission: Methodology and Application, Springer International Publishing, Cham, Switzerland 2017, pp. 29–71.
[134] A. Wade, R. Copley, B. Clarke, A. Alsheikh Omar, A.R. Beadling, T. Liskiewicz, M.G. Bryant, Real-time fretting loop regime transition identification using acoustic emissions, Tribol. Int. 145 (2020) 106149.
[135] S.K. Al-Jumaili, M.R. Pearson, K.M. Holford, M.J. Eaton, R. Pullin, Acoustic emission source location in complex structures using full automatic delta T mapping technique, Mech. Syst. Signal Process. 72–73 (2016) 513–524.
[136] M.R. Pearson, M. Eaton, C. Featherston, R. Pullin, K. Holford, Improved acoustic emission source location during fatigue and impact events in metallic and composite structures, Struct. Health Monit. 16 (4) (2017) 382–399.
[137] Z. Nazarchuk, V. Skalskyi, O. Serhiyenko, Analysis of acoustic emission caused by internal cracks, Acoustic Emission: Methodology and Application, Springer, Cham 2017, pp. 75–105.
[138] M. Kubota, Y. Tanaka, Y. Kondo, Fretting fatigue strength of SCM435H steel and SUH660 heat-resistant steel in hydrogen gas environment, Tribo Test 14 (3) (2008) 177–191.
[139] M. Kubota, Y. Tanaka, Y. Kondo, The effect of hydrogen gas environment on fretting fatigue strength of materials used for hydrogen utilization machines, Tribol. Int. 42 (9) (2009) 1352–1359.
[140] C.K. Mukhopadhyay, T. Jayakumar, T.K. Haneef, S. Suresh Kumar, B.P.C. Rao, S. Goyal, S.K. Gupta, V. Bhasin, S. Vishnuvardhan, G. Raghava, P. Gandhi, Use of acoustic emission and ultrasonic techniques for monitoring crack initiation/growth during ratcheting studies on 304LN stainless steel straight pipe, Pressure Vessels Piping 116 (2014) 27–36.
[141] R. Urbanek, J. Bar, Influence of motion compensation on lock-in thermographic investigations of fatigue crack propagation, Eng. Fract. Mech. 183 (2017) 13–25.
[142] P. Liu, H. Sohn, T. Kundu, S. Yang, Noncontact detection of fatigue cracks by laser nonlinear wave modulation spectroscopy (LNWMS), NDT E Int. 66 (2014) 106–116.
[143] H. Proudhon, S. Fouvry, J.Y. Buffière, A fretting crack initiation prediction taking into account the surface roughness and the crack nucleation process volume, Int. J. Fatigue 27 (2005) 569–579.
[144] Y.K. An, B. Park, H. Sohn, Complete noncontact laser ultrasonic imaging for automated crack visualization in a plate, Smart Mater. Struct. 22 (2) (2013) (pp. 25022–10).
[145] J. Camacho, D. Atehortua, J.F. Cruza, J. Brizuela, J. Ealo, Ultrasonic crack evaluation by phase coherence processing and TFM and its application to online monitoring in fatigue tests, NDT E Int. 93 (2018) 164–174.
[146] T.P. Chapman, K.M. Kareh, M. Knop, T. Connolley, P.D. Lee, M.A. Azeem, D. Rugg, T.C. Lindley, D. Dye, Characterisation of short fatigue cracks in titanium alloy IMI 834 using X-ray microtomography, Acta Materialia 99 (2015) 49–62 aug.
[147] S.T. Carter, J. Rotella, R.F. Agyei, X. Xiao, M.D. Sangid, Measuring fatigue crack deflections via cracking of constituent particles in AA7050 via in situ x-ray synchrotron-based micro-tomography, Int. J. Fatigue 116 (2018) 490–504.
[148] M. Waddell, K. Walker, R. Bandyopadhyay, K. Kapoor, A. Mallory, X. Xiao, A.C. Chuang, Q. Liu, N. Phan, M.D. Sangid, Small fatigue crack growth behavior of Ti-6Al-4V produced via selective laser melting: In situ characterization of a 3D crack tip interactions with defects, Int. J. Fatigue 137 (2020) 105638 apr.
[149] E. Ferrié, J.Y. Buffière, W. Ludwig, A. Gravouil, L. Edwards, Fatigue crack propagation: In situ visualization using X-ray microtomography and 3D simulation using the extended finite element method, Acta Materialia 54 (2006) 1111–1122 feb.
[150] C. Verdu, J. Adrien, J.Y. Buffière, Three-dimensional shape of the early stages of fatigue cracks nucleated in nodular cast iron, Mater. Sci. Eng. A 483–484 (2008) 402–405 jun.
[151] S. Birosca, J.Y. Buffiere, F.A. Garcia-Pastor, M. Karadge, L. Babout, M. Preuss, Threedimensional characterization of fatigue cracks in Ti-6246 using X-ray tomography and electron backscatter diffraction, Acta Materialia 57 (2009) 5834–5847 nov.
[152] B. Masserey, P. Fromme, In-situ monitoring of fatigue crack growth using high frequency guided waves, NDT E Int. 71 (2015) 1–7.
[153] J. Jiao, H. Lv, C. He, B. Wu, Fatigue crack evaluation using the non-collinear wave mixing technique, Smart Mater. Struct. 26 (2017) 1–11.
[154] J. Camacho, M. Parrilla, C. Fritsch, Phase coherence imaging, IEEE Trans. Ultrason. Ferroelectr. Freq. Control 56 (5) (2009) 1403–1404.
[155] D. Krewerth, T. Lippmann, A. Weidner, H. Biermann, Application of full-surface view in situ thermography measurements during ultrasonic fatigue of cast steel G42CrMo4, Int. J. Fatigue 80 (2015) 459–467.

[156] D. Wagner, N. Ranc, C. Bathias, P.C. Paris, Fatigue crack initiation detection by an infrared thermography method, Fatigue Fract. Eng. Mater. Struct. 33 (1) (2010) 12–21.
[157] R.H. Talemi, S. Chhith, W. De Waele, Experimental and numerical study on effect of forming process on low-cycle fatigue behaviour of high-strength steel, Fatigue Fract. Eng. Mater. Struct. 40 (2017) 2050–2067.
[158] T. Naoe, Z. Xiong, M. Futakawa, Temperature Measurement for In-Situ Crack Monitoring under High-Frequency Loading, 2017.
[159] B. Weekes, D.P. Almond, P. Cawley, T. Barden, Eddy-current induced thermography - probability of detection study of small fatigue cracks in steel, titanium and nickel-based superalloy, NDT E Int. 49 (2012) 47–56.
[160] M. He, L. Zhang, W. Zheng, Y. Feng, Crack detection based on a moving mode of eddy current thermography method, Measurement 109 (2017) 119–129.
[161] M. Chai, J. Zhang, Z. Zhang, Q. Duan, G. Cheng, Acoustic emission studies for characterization of fatigue crack growth in 316LN stainless steel and welds, Appl. Acoust. 126 (2017) 101–113.
[162] M. Chai, Q. Duan, X. Hou, Z. Zhang, L. Li, Fracture toughness evaluation of 316LN stainless steel and weld using acoustic emission technique, ISIJ Int. 56 (5) (2016) 875–882.
[163] Z. Bo, Z. Yanan, C. Changzheng, Acoustic emission detection of fatigue cracks in wind turbine blades based on blind deconvolution separation, Fatigue Fract. Eng. Mater. Struct. 40 (2016) 959–970.
[164] T.M. Roberts, M. Talebzadeh, Fatigue life prediction based on crack propagation and acoustic emission count rates, J. Constr. Steel Res. 59 (2003) 679–694.
[165] V. Zilberstein, D. Schlicker, K. Walrath, V. Weiss, N. Goldfine, MWM eddy current sensors for monitoring of crack initiation and growth during fatigue tests and in service, Int. J. Fatigue 23 (2001) 477–485.
[166] V. Zilberstein, K. Walrath, D. Grundy, D. Schlicker, N. Goldfine, E. Abramovici, T. Yentzer, MWM eddy-current arrays for crack initiation and growth monitoring, Int. J. Fatigue 25 (2003) 1147–1155.
[167] S. Jiao, L. Cheng, X. Li, P. Li, H. Ding, Monitoring fatigue cracks of a metal structure using an eddy current sensor, EURASIP J. Wirel. Commun. Netw. 188 (2016) 1–14.
[168] R. Xie, D. Chen, M. Pan, W. Tian, X. Wu, W. Zhou, Y. Tang, Fatigue crack length sizing using a novel flexible eddy current sensor array, Sensors (Switzerland) 15 (12) (2015) 32138–32151.
[169] B. Pan, K. Qian, H. Xie, A. Asundi, Two-dimensional digital image correlation for in-plane displacement and strain measurement: a review, Meas. Sci. Technol. 20 (2009) 062001.
[170] J. Zhao, Y. Sang, F. Duan, The state of the art of two-dimensional digital image correlation computational method, Eng. Reports 1 (2019) 1–15 sep.
[171] J. Juoksukangas, A. Lehtovaara, A. Mäntylä, A comparison of relative displacement fields between numerical predictions and experimental results in fretting contact, Proceed. Instit. Mechan. Eng. Part J 230 (10) (2016) 1273–1287.
[172] J. Winkler, C.T. Georgakis, G. Fischer, Fretting fatigue behavior of high-strength steel monostrands under bending load, Int. J. Fatigue 70 (2015) 13–23.
[173] C. Jiménez-Peña, R.H. Talemi, B. Rossi, D. Debruyne, Investigations on the fretting fatigue failure mechanism of bolted joints in high strength steel subjected to different levels of pre-tension, Tribol. Int. 108 (2017) 128–140.
[174] V. Venugopal Poovakaud, C. Jiménez-Peña, R. Talemi, S. Coppieters, D. Debruyne, Assessment of fretting fatigue in high strength steel bolted connections with simplified Fe modelling techniques, Tribol. Int. 143 (2020) 106083 mar.
[175] M. Nesládek, M. Španiel, J. Jurenka, J. Růžička, J. Kuželka, Fretting fatigue - experimental and numerical approaches, Int. J. Fatigue 44 (2012) 61–73.
[176] J. Juoksukangas, A. Lehtovaara, A. Mäntylä, Applying the digital image correlation method to fretting contact for slip measurement, Proceed. Inst. Mech. Eng. Part J 231 (4) (2017) 509–519.
[177] J. De Pauw, W. De Waele, R. Hojjati-Talemi, P. De Baets, On the use of digital image correlation for slip measurement during coupon scale fretting fatigue experiments, Int. J. Solids Struct. 51 (18) (2014) 3058–3066.
[178] J. Rupil, S. Roux, F. Hild, L. Vincent, Fatigue microcrack detection with digital image correlation, J. Strain Anal. Eng. Des. 46 (6) (2011) 492–509.
[179] S. Vanlanduit, J. Vanherzeele, R. Longo, P. Guillaume, A digital image correlation method for fatigue test experiments, Opt. Lasers Eng. 47 (3–4) (2009) 371–378.
[180] Y.J. Yin, W. He, H.M. Xie, L.F. Wu, High-temperature fatigue crack propagation study of superalloy GH4169 by single-lens 3D digital image correlation, Sci. China Technol. Sci. 63 (4) (2020) 693–704.
[181] T. Thäsler, J. Holtmannspötter, H.J. Gudladt, Monitoring the fatigue crack growth behavior of composite joints using in situ 2D-digital image correlation, J. Adhes. 95 (5–7) (2019) 595–613.
[182] J. Tong, Full-field characterisation of crack tip deformation and fatigue crack growth using digital image correlation—a review, Fatigue Fract. Eng. Mater. Struct. 41 (9) (2018) 1855–1869.
[183] M. Mokhtarishirazabad, P. Lopez-Crespo, M. Zanganeh, Stress intensity factor monitoring under cyclic loading by digital image correlation, Fatigue Fract. Eng. Mater. Struct. 41 (10) (2018) 2162–2171.
[184] F. Mathieu, F. Hild, S. Roux, Identification of a crack propagation law by digital image correlation, Int. J. Fatigue 36 (2012) 146–154 mar.
[185] M. Mostafavi, T. Marrow, Quantitative in situ study of short crack propagation in polygranular graphite by digital image correlation, Fatigue Fracture Eng. Mater. Struct. 35 (2012) 695–707 aug.
[186] L. De Chiffre, S. Carmignato, J.P. Kruth, R. Schmitt, A. Weckenmann, Industrial applications of computed tomography, CIRP Ann. Manuf. Technol. 63 (2) (2014) 655–677.
[187] M. Poncelet, G. Barbier, B. Raka, S. Courtin, R. Desmorat, J.C. Le-Roux, L. Vincent, Biaxial high cycle fatigue of a type 304L stainless steel: Cyclic strains and crack initiation detection by digital image correlation, Eur. J. Mech. A/Solids 29 (2010) 810–825 sep.